

RESEARCH ARTICLE | *Higher Neural Functions and Behavior*

Pupil-linked arousal modulates behavior in rats performing a whisker deflection direction discrimination task

Brian J. Schriver, Svetlana Bagdasarov, and Qi Wang

Department of Biomedical Engineering, Columbia University, New York, New York

Submitted 1 May 2018; accepted in final form 9 July 2018

Schriver BJ, Bagdasarov S, Wang Q. Pupil-linked arousal modulates behavior in rats performing a whisker deflection direction discrimination task. *J Neurophysiol* 120: 1655–1670, 2018. First published July 11, 2018; doi:10.1152/jn.00290.2018.—Non-luminance-mediated changes in pupil size have been widely used to index arousal state. Recent animal studies have demonstrated correlations between behavioral state-related pupil dynamics and sensory processing. However, the relationship between pupil-linked arousal and behavior in animals performing perceptual tasks has not been fully elucidated. In the present study, we trained head-fixed rats to discriminate between directions of whisker movements using a Go/No-Go discrimination paradigm while imaging their pupils. Reaction times in this discrimination task were significantly slower than in previously reported detection tasks with similar setup, suggesting that discrimination required an increased cognitive load. We found the pupils dilated for all trials following stimulus presentation. Interestingly, in correct rejection trials, where pupil dilations solely resulted from cognitive processing, dilations were larger for more difficult stimuli. Baseline pupil size before stimulus presentation strongly correlated with behavior, as perceptual sensitivity peaked at intermediate pupil baselines and reaction time was fastest at large baselines. We further explored these relationships by investigating to what extent pupil baseline was predictive of upcoming behavior and found that a Bayesian decoder had significantly greater-than-chance probability in correctly predicting behavioral outcomes. Moreover, the outcome of the previous trial showed a strong correlation with behavior on present trials. Animals were more liberal and faster in responding following hit trials, whereas perceptual sensitivity was greatest following correct rejection trials. Taken together, these results suggest a tight correlation between pupil dynamics, perceptual performance, and reaction time in behaving rats, all of which are modulated by fluctuating arousal state.

NEW & NOTEWORTHY In this study, we for the first time demonstrated that head-fixed rats were able to discriminate different directions of whisker movement. Interestingly, we found that the pupil dilated more when discriminating more difficult stimuli, a phenomenon reported in human subjects but not in animals. Baseline pupil size before stimulus presentation was found to strongly correlate with behavior, and a Bayesian decoder had significantly greater-than-chance probability in correctly predicting behavioral outcomes based on the baseline pupil size.

arousal; discrimination task; pupil dynamics; signal detection theory; whisker system

INTRODUCTION

A fundamental question in systems neuroscience is how behavioral state modulates information processing in the brain (Harris and Thiele 2011; Lee and Dan 2012; McCormick et al. 2015; McGinley et al. 2015b; Steriade et al. 1993). Behavioral state, including arousal, attention, and movement, imposes heavy modulatory effects on neural coding, perception, and behavioral performance (Cano et al. 2006; Musall et al. In press; Niell and Stryker 2010; Polack et al. 2013; Poulet and Petersen 2008; Stringer et al. In press). Seminal work in human subjects, by Hess and Polt (1960), demonstrated a tight correlation between non-luminance-induced pupil dilation and emotional arousal mediated by sex-specific interests. Since then, non-luminance-induced changes in pupil size have been widely used to index arousal state (i.e., pupil-linked arousal) in human behavior (Colizoli et al. In press; de Gee et al. 2014; Eldar et al. 2013; Hong et al. 2014; Nassar et al. 2012; Urai et al. 2017). For example, Urai et al. (2017) reported that heightened pupil-linked arousal was likely to result in a higher tendency of human subjects to alternate their choice on the subsequent trial when performing a perceptual decision task. Furthermore, several recent animal studies revealed that non-luminance-induced changes in pupil size can be used to track the fluctuation of cortical arousal and cognitive factors (Ebitz et al. 2014; Lee and Margolis 2016; McGinley et al. 2015a; Reimer et al. 2014; Varazzani et al. 2015; Vinck et al. 2015) [for a review, see Larsen and Waters (2018)], suggesting that the correlation between pupil size and behavioral state is a universal phenomenon across mammalian species. Therefore, further pupillometry studies in animal models may provide insight into neural circuitry mediating the relationship between pupil-linked arousal and information processing in the brain.

The rodent vibrissa system has evolved into a sophisticated sensory system (Diamond et al. 2008). In their natural environment, rodents use their whiskers to feel objects of interest, resulting in each whisker undergoing complex motion in different directions depending on the shape and surface properties of the object (Berg and Kleinfeld 2003; Brecht et al. 1997; Hartmann et al. 2003; Jadhav et al. 2009; Ritt et al. 2008; Wolfe et al. 2008), suggesting that the direction of whisker movement is an important tactile cue. Indeed, in the vibrissa pathway, electrophysiology recordings showed that sensory neurons exhibited sensitivity to the direction of whisker movement in the trigeminal ganglion (Lichtenstein et al. 1990), trigeminal nuclei (Furuta et al. 2006; Kaloti et al. 2016),

Address for reprint requests and other correspondence: Q. Wang, Dept. of Biomedical Engineering, Columbia Univ., ET 351, 500 W. 120th St., New York, NY 10027 (e-mail: qi.wang@columbia.edu).

thalamus (Bale and Petersen 2009; Hartings et al. 2000), and barrel cortex (Andermann and Moore 2006; Bruno et al. 2003; Vilarchao et al. 2018; Wilent and Contreras 2005). However, the functional consequences of these tuning properties in behavior have not been systematically tested yet.

In perceptual tasks, upon the arrival of a sensory stimulus, the animal must take time to accumulate available evidence and plan to execute or withhold a motor action to indicate choice (Brunton et al. 2013; Delis et al. 2018; Gold and Shadlen 2007; Gomez et al. 2007). The reaction time, the time elapsed between stimulus presentation and an action, is also affected by behavioral state (Mauri et al. 2015; Moradi et al. 2007; Zhang et al. 2012). For example, by manipulating subjects' arousal level through transcranial electrical stimulation, Mauri et al. (2015) showed reduction in reaction time in detecting a target stimulus with increase of arousal, measured by skin conductance. However, the extent to which pupil dynamics covary with reaction time in behavior remains poorly understood (Gilzenrat et al. 2010; Hong et al. 2014; Murphy et al. 2011).

In the present study, we hypothesize that the behavior of rats performing a tactile discrimination task is highly dependent on the level of arousal, which can be indexed by pupil dynamics. Using a Go/No-Go paradigm, we trained head-fixed rats to discriminate between two opposing directions of single right whisker deflections while imaging their left pupil. The pupil dilated following stimulus presentation in all trials. Similar to human subjects, stimuli harder to discriminate resulted in larger pupil dilations. The dependence of behavioral outcomes on fluctuating prestimulus pupil size allowed a Bayesian decoder to predict behavior based on pupil size at a significantly higher than chance level. Taken together, our results suggest a tight correlation between pupil dynamics, perceptual performance, and reaction time, all of which are influenced by fluctuating behavioral state.

MATERIALS AND METHODS

All experimental procedures were approved by the Columbia University Institutional Animal Care and Use Committee and were conducted in compliance with NIH guidelines. Behavioral studies were conducted using five female albino rats (Sprague-Dawley, Charles River Laboratories, Wilmington, MA; ~225–275 g at time of implantation). Animals were single housed after implantation in a dedicated housing facility, which maintained a 12-h:12-h light/dark cycle. All behavioral tasks were conducted in the light phase in a light attenuation chamber.

Surgical Implantation

All animals used in the behavioral task were habituated to experimenters for a minimum of 10 days before undergoing surgical procedures to implant a head post or head plate (Schwarz et al. 2010). The head posts consisted of stainless steel screws implanted with the threaded ends facing upward (Ollerenshaw et al. 2014; Stütgen and Schwarz 2008), whereas the head plates consisted of custom-made aluminum plates that allowed for head fixation using bilateral pneumatic actuators affixed to a custom restraint box to allow for neural recording and manipulation in future studies (Scott et al. 2013).

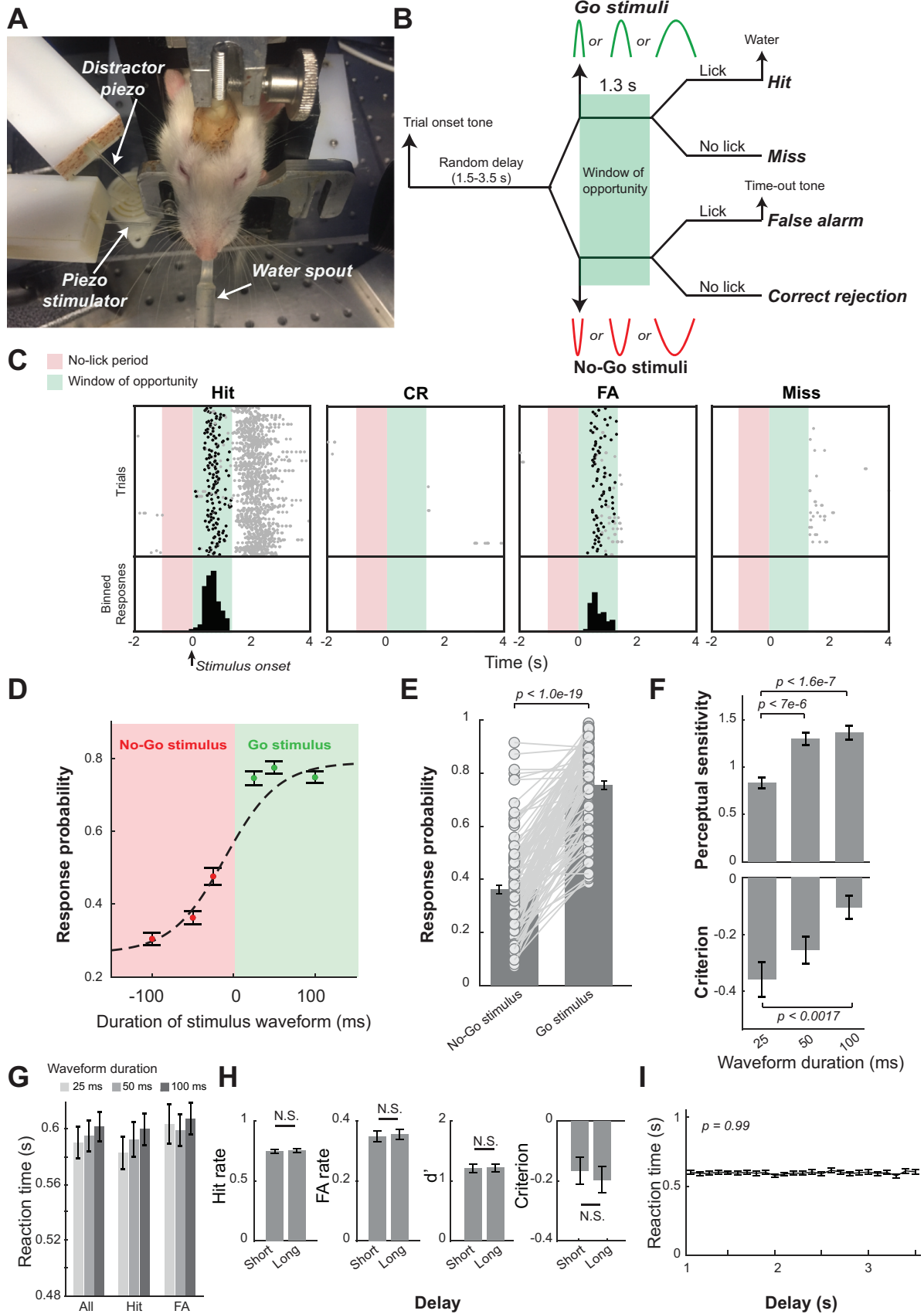
In aseptic surgeries, anesthesia was induced with a ketamine/xylozine cocktail (80/5 mg/kg ip) or isoflurane (1.5–3.0% with a nose cone). The depth of anesthesia was periodically monitored through reflexes to aversive stimuli (toe or tail pinch) and a continuous

measurement of heart rate and blood oxygenation was monitored using a pulse oximeter (Nonin, Plymouth, MN). Ophthalmic ointment was immediately applied to the eyes after anesthetics took effect to prevent drying. After the scalp was shaved and hair was removed with depilatory cream, animals were placed in a stereotaxic device using nonpenetrating ear bars (RWD Life Science, Shenzhen, China). The body temperature was maintained at 37°C throughout the procedure using a feedback-controlled heating pad (FHC, Bowdoinham, ME). Atropine (0.05 mg/kg ip) and buprenorphine (Buprenex, 0.03 mg/kg sc) were administered to keep the lungs clear of fluid and as an analgesic, respectively. Two milliliters of Ringer's solution (subcutaneously to the back) was also administered to prevent dehydration. Alcohol and a 10% povidone-iodine solution were alternately used three times to clean the scalp. After exposing and cleaning the skull, we drilled six to nine burr holes in the skull, and we inserted stainless steel screws (0–80 thread; McMaster Carr, Robbinsville, NJ) to anchor the implant (Schwarz et al. 2010). The center of the head post or head plate was then stereotaxically positioned ~1 mm posterior to the lambda, after which dental cement was applied, anchoring the implant to the bone screws (Paxinos et al. 1985; Schwarz et al. 2010). The wound was then closed with surgical sutures and treated with antibiotic ointment. Antibiotics (Baytril, 5 mg/kg sc) and extra analgesics (ketoprofen, 5 mg/kg sc) were administered for a minimum of 5 days postoperatively. The animals began water restriction and subsequent training following 10 days of recovery from implantation surgery.

Behavioral Procedures

Behavioral apparatus. The head-fixation behavioral apparatus was contained in a standard sound and light attenuation chamber (Med Associates, St. Albans, VT). During training, the animals were head-fixed within one of two custom-built restraint boxes. If they had been implanted with a head post ($n = 4$), the box resembled that described in Ollerenshaw et al. (2014). If they had been implanted with a head plate ($n = 3$), the box was similar to that described in Scott et al. (2013), where the animals entered the box from the back and placed their head plates into a slot in the front. Two pneumatic cylinders on either side of the head that were fixed with ball bearings aligned with grooves in the custom-made head plate to rigidly hold the animals' heads. A foot pedal was used to quickly switch on or off a pneumatic valve that regulated the pressure of compressed air. The restraint box was rigidly attached to the floor of the chamber. A 1-ml syringe body was mounted to a flexible beam and placed directly in front of the animal. This served both to deliver water rewards and to measure licking responses via a piezoelectric force sensor bonded to the flexible beam. Bending of the beam attributable to licking typically resulted in an ~50-mV voltage swing across the output of the sensor, which was connected to an A/D channel of a DAQ card (PCI-6259; National Instruments, Dallas, TX).

Precise tactile stimuli (i.e., whisker movements) were delivered using a multilayer piezoelectric bending actuator (PL140; Physik Instrumente, Karlsruhe, Germany) driven by a high-voltage amplifier (OPA452; Texas Instruments, Dallas, TX). To precisely deflect a whisker, a short capillary tube (capillary glass pipette ~15.0 mm long with 1.0-mm outer diameter and 0.5-mm inner diameter; A-M Systems, Carlsborg, WA) was bonded to the end of the piezo bending actuator (Fig. 1A). The capillary tube was placed ~8 mm away from the right snout, and a single whisker of the head-fixed animal was placed inside the capillary tube. For each animal, we chose the thickest of the C2, C3, or D2 macrovibrissae (to minimize time to insert the whisker into the stimulator pipette), and this whisker was subsequently stimulated for all sessions. Surrounding whiskers were not trimmed. The piezo stimulation was oriented such that the whisker could be deflected in the dorsal-ventral direction. A second identical piezoelectric bending actuator with capillary tube was placed near the first whisker stimulator but did not have contact with any whiskers.



This “distractor whisker stimulator” was programmed to deliver identical stimulus patterns at random time points, designed to prevent the animal from cueing off the sound of the moving capillary tube during the behavioral task. To further mask possible auditory cues, a white noise-masking stimulus (~75 dB) was delivered through a buzzer (bandwidth: 16 Hz–10 kHz) installed in front of the animal next to the whisker manipulator.

A speaker was installed within the chamber to deliver onset (6.0 kHz), reward (3.0 kHz), and timeout tones (16.5 kHz). The interior of the behavioral chamber was illuminated with an infrared LED, and the animal was remotely monitored with a CCD camera (The Imaging Source, Charlotte, NC) during the task. Control of the behavioral task and sampling of animals’ behavioral responses were performed by custom-programmed software running on a MATLAB xPC target real-time system (MathWorks, Natick, MA). All behavioral data were sampled at 1 kHz and logged for offline analyses.

Tactile stimulus. Whisker deflections with half-sinusoidal waveforms (3 durations: 25, 50, and 100 ms) (Fig. 1B) in the dorsal direction were randomly designated as Go stimuli, whereas identical whisker deflections but in the ventral direction were randomly designated as No-Go stimuli. The probability of each waveform being presented was set to be the same. The peak whisker deflection was ~2 mm, calibrated using a laser micrometer (Metralight, Burlingame, CA), resulting in mean whisker deflection velocities of ~1,200, 600, and 300°/s for the three waveforms, respectively. The minimum whisker deflection velocity was above the detection threshold of whisker deflection reported previously (Ollerenshaw et al. 2014; Stüttgen and Schwarz 2008).

Pupillometry recording. Recording of the pupil contralateral to the whisker deflection was made using pupillometry systems assembled in house (FL3-U3-13Y3M-C; FLIR, Richmond, BC, Canada) (Liu et al. 2017), which were triggered at 10 Hz by the xPC target real-time system (MathWorks) that controlled the behavioral task. Pupil images were streamed to a high-speed solid-state drive for offline analysis, which was performed using MATLAB. At the beginning of each session before any tasks, we adjusted the ambient luminance in the chamber to make the pupil size an intermediate level (Fig. 2A), which allowed the pupil to fluctuate over a dynamic range. For each video clip, a region of interest (ROI) was first manually assigned. The histogram of pixel intensity within the ROI was then calculated to estimate the optimal threshold for pupil segmentation (Liu et al. 2017). Pupil contour was segmented using the threshold, and pupil size was defined as the area within the contour (Fig. 2A). Approximately 5% of segmented images were randomly selected for visual inspection to ensure the accuracy of automatic segmentation. Pupil size during periods of blinks was derived by linearly interpolating pupil sizes preceding and after blinks (Nassar et al. 2012).

Training and the Go/No-Go discrimination task. Water deprivation schedule and procedures of head-fixation habituation were described in detail previously (Ollerenshaw et al. 2014). Briefly, to motivate animals during the tasks, access to water was restricted, i.e., animals did not have access to water in their home cages on training days. However, during the behavioral task, correct responses to a Go stimulus were rewarded with ~60- μ l aliquots of Kool-Aid water, and they were allowed to continue performing the task until satiated. During nontraining days, animals were given ad libitum access to

water. The weight of the animals was measured and logged immediately after the task.

After the animals were placed on a water-restriction schedule, they were systematically habituated to head-fixation and trained to perform the full Go/No-Go discrimination task. In this Go/No-Go discrimination paradigm, we randomly designated whisker deflections in the dorsal direction as Go stimuli (S+ stimuli) and whisker deflections in the ventral direction as No-Go stimuli (S- stimuli) for all animals used in this study. The onset of each trial was indicated by a brief trial onset tone (300 ms, 6 kHz). Between the trial onset tone and the stimulus presentation, the animal had to wait for a period of random length selected from a 1.0- to 3.5-s uniform distribution. To discourage the animal from impulsively licking, the last 1 s of the waiting period was a designated “no lick” period during which any premature licks resulted in an additional delay in stimulus presentation pulled from a 1.0- to 2.5-s uniform distribution. The stimulus for each trial could be either a Go stimulus or a No-Go stimulus (equal probability). Licking within a window of opportunity (1.3 s) following a Go stimulus resulted in a brief reward tone (300 ms, 3 kHz) accompanied by administration of Kool-Aid water (~60 μ l), whereas licking within the window of opportunity following a No-Go stimulus triggered a timeout tone (5 s, 16.5 kHz), which began a 10-s timeout period. Correct rejection (CR) and miss outcomes had no consequences (i.e., not rewarded or penalized). A 6-s intertrial period followed the end of the window of opportunity for CR trials and miss trials, water reward for hit trials, and timeout period for false alarm (FA) trials. The animals were considered experts once they achieved higher hit rate (HR) than FA rate (FAR) for five sessions in a row. It took 37, 27, 23, 46, and 16 sessions for the five animals, respectively. On rare occasions, expert rats performed poorly in some sessions, resulting in a negative perceptual sensitivity (i.e., FAR was greater than HR). We included these sessions in the analyses. However, all results held if we excluded sessions with negative perceptual sensitivities. Across all five animals, 111 sessions (a total of 38,249 trials) were recorded.

Data Analysis

All data analyses were first conducted on individual sessions. Grand averages and standard errors of means were then calculated across sessions for analysis and presentation. For each session, the first 20 trials were excluded because of the time required to adjust the pupillometry camera.

Behavioral performance. Response probabilities for each session were calculated as the HR (i.e., number of hit trials/number of S+ trials) and FAR (i.e., number of FA trials/number of S- trials). These were used to calculate perceptual sensitivity (d') and decision criterion as

$$d' = \Psi^{-1}(\text{Hit rate}) - \Psi^{-1}(\text{FA rate}) \quad (1)$$

$$\text{Criterion} = -[\Psi^{-1}(\text{Hit rate}) + \Psi^{-1}(\text{FA rate})]/2$$

where Ψ^{-1} is inverse of the cumulative Gaussian distribution.

Response probabilities were also calculated dependent on stimulus durations, with HRs, FARs, d' s, and criterions calculated independently for each subset of trials with stimuli of given durations in either the dorsal (S+) or ventral (S-) direction. For analyzing response probabilities, perceptual sensitivity, and decision criterion vs. percent-

Fig. 1. Behavioral performance of head-restrained rats performing a whisker deflection direction discrimination task. A: behavioral training setup. B: Go/No-Go discrimination paradigm with stimuli of 15° of deflection, with 25-, 50-, and 100-ms durations. C: example lick raster plots separated by response type showing licks (black dots indicate the first lick within the window of opportunity). Red zone indicates the no-lick period, and green zone indicates the window of opportunity. D: psychometric curves averaged across sessions. E: response probability to Go stimuli and No-Go stimuli across sessions. F: duration of stimulus waveform had significant effects on animals’ perceptual sensitivity [$P < 6.4 \times 10^{-8}$, $F(2,329) = 37.44$] and decision criterion [$P < 0.003$, $F(2,329) = 6.03$, 1-way ANOVA test]. G: duration of stimulus waveform had no effects on reaction time. H: behavior appeared independent of delay preceding stimulus onset, comparing short (less than mean delay) to long delays (greater than mean delay). I: average reaction times within 0.1-s bins across the entire window of possible delays suggested that delay preceding stimulus onset had no effects on reaction time. Error bars indicate SE. CR, correct rejection; FA, false alarm.

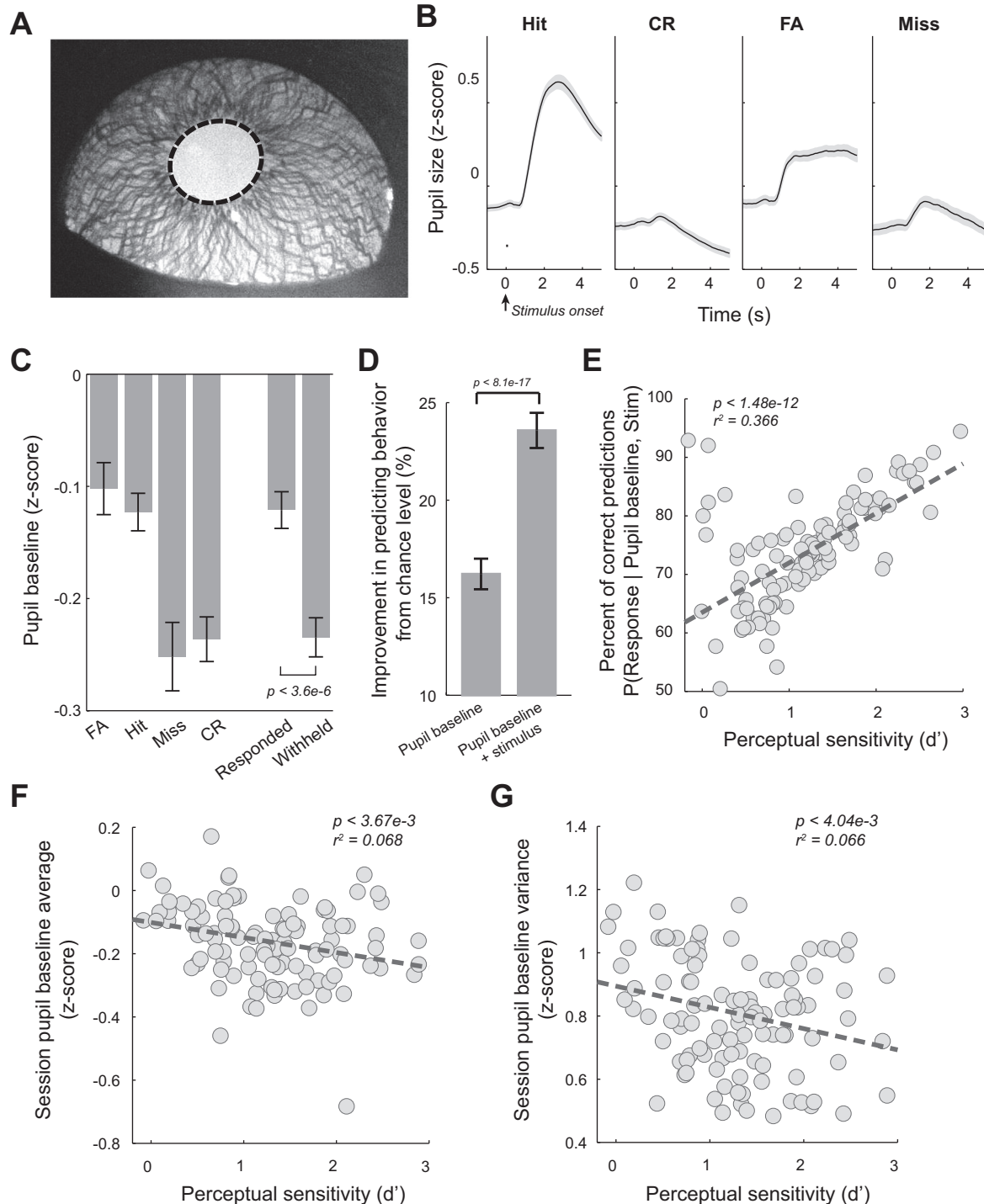


Fig. 2. Pupil dynamics during the tactile discrimination task. **A**: example pupil image with overlaid pupil contour (dashed). **B**: average pupil dynamics around stimulus presentation for the 4 behavioral outcomes across all sessions of the 5 animals. **C**: pupil baselines for the 4 behavioral outcomes averaged across sessions. **D**: prestimulus pupil size was predictive of behavior. **E**: percentage of correct prediction of behavior based on pupil baseline and stimulus identity was correlated with perceptual performance. **F**: pupil baseline average was negatively correlated with perceptual performance. **G**: within-session pupil baseline variance was negatively correlated with perceptual performance. Error bars and shaded areas indicate SE. CR, correct rejection; FA, false alarm.

age of maximum baseline, the baseline range of each session was first computed and then evenly broken into 20 bins, each trial was sorted into one of the bins, and HR, FAR, d' , and criterion were calculated for each bin. Calculating d' and criterion is not possible when HR or FAR equal 0 or 1. Therefore, the loglinear approach was utilized to allow for calculating d' and criterion in bins where HR or FAR equaled 0 or 1, which involves adding 0.5 to the number of hits and

FAs and 1 to the number of S+ and S- presentations before calculating HR and FAR (Stanislaw and Todorov 1999).

Reaction times were computed as the time from stimulus onset, as this is when the window of opportunity began, until the first lick response within the window of opportunity. Reaction times were only computed when a response was logged in the window of opportunity, i.e., for hit and FA trials, but not miss trials or CR trials. To determine

whether behavioral performance was affected by the randomized delay (1.0–3.5 s) between the trial onset and stimulus delivery, the average delay was calculated for each session. HR, FAR, d' , and criterion were then calculated for all trials with a delay below average (i.e., 2.25 s) (Short) or above average (Long). To determine whether there were any effects on reaction time, the delay period was broken into 25 bins, and the average reaction time for each bin was calculated for each session.

Pupil dynamics. Pupil sizes were Z-scored for each session ($Z\text{-score} = \frac{\text{pupil size} - \text{mean}}{\text{SD}}$) before further analyses. Because impulsive licks (licks before stimulus presentation) or late licks (licks after the window of opportunity closed in CR or miss trials) may dilate pupil and bias pupil baseline analysis, we excluded trials with impulsive and/or late licks (16.06% of total trials) in pupil dynamics analyses (inclusion of these trials did not change the reported findings). Pupil sizes were aligned by stimulus onset. Stereotypical pupil responses for each behavioral outcome were calculated as the average pupil size at each time point 0.5 s preceding stimulus onset to 4.5 s following stimulus onset. Average baselines and dilations were calculated from these averaged stereotypical responses for each behavioral outcome for each session. Baseline pupil sizes were computed as the average of the pupil sizes in the 0.5 s preceding the stimulus, whereas dilations were calculated as the maximum pupil size in the 4.5 s following stimulus minus the baseline. To calculate the percentage of maximum pupil baseline, all baselines were normalized for each session.

% of Maximum Pupil Baseline

$$= \frac{|\text{Pupil Baseline}_t - \text{Pupil Baseline}_{\text{minimum}}|}{|\text{Pupil Baseline}_{\text{maximum}} - \text{Pupil Baseline}_{\text{minimum}}|} \quad (2)$$

To visualize fluctuations of pupil and behavior in single sessions, average Z-scored pupil size was calculated for every trial. A sliding window was used to calculate HR, FAR, d' , criterion, average pupil baseline, and average reaction times for every 30 trials within each session (a sliding window of 20 trials yielded similar results for all analyses involving a sliding window, $P < 0.05$). Correlation analysis was conducted by calculating the Pearson's correlation coefficient for each session. For the estimation of the relationship between pupil baseline and behavioral performance, a sliding window was used to calculate d' and criterion as well as average pupil baseline and dilation for every 30 trials within each session. The Pearson's correlation coefficients comparing each behavioral aspect to each pupil dynamic were then calculated and averaged across sessions. To determine the correlation between pupil baseline and dilation on a single trial basis, these values were computed by the Pearson's correlation coefficient, which were then averaged across sessions.

Reaction time analysis. For analyzing response probabilities, perceptual sensitivity, decision criterion, and pupil baseline vs. percentage of maximum reaction time, a 30-trial sliding window was used. The average reaction time within sliding windows was used to map perceptual sensitivity/decision criterion to percentage of maximum normalized reaction time of the session. More specifically, the range of average reaction times (calculated using sliding windows) for each session was broken into 20 bins, then each window was sorted into one of the bins, and then HR, FAR, d' , and criterion were averaged within each bin. The loglinear approach described above was used when necessary in computing d' and decision criterion, whereas, for pupil baseline, bins without values were excluded. To determine the relationship between reaction time and pupil dynamics, average hit and FA reaction times were computed for each session. All hit trials were then sorted into slow (i.e., reaction time $>$ mean hit reaction time) or fast (i.e., reaction time $<$ mean hit reaction time), and an average slow and fast pupil response was found for each session. Baselines and dilations were calculated from these. The same procedures were conducted for FA trials.

Prior Response Analysis

Average pupil dynamics were calculated for time courses (0.5 s preceding stimulus onset to 4.5 s following stimulus onset) for each behavioral outcome conditioned on the previous outcome. Baselines were calculated from these averages. HR, FAR, perceptual sensitivity, decision criterion, and average reaction times were also calculated conditioned on the outcome of the previous trial. The loglinear strategy described above was again used when necessary in computing d' and decision criterion.

Bayesian Inference Prediction

Maximum a posteriori (MAP) estimation was utilized to predict the behavioral outcome based on only baseline pupil size or a combination of baseline pupil size and the stimulus presented. To infer behavioral outcome based only on baseline pupil sizes, the probabilities used for the Bayesian inference were computed as (Bishop 2006)

$$P(\text{Resp} | \text{PA}) \propto P(\text{PA} | \text{Resp}) * P(\text{Resp}) \quad (3)$$

We also computed the probabilities for responses based on baseline pupil sizes and stimulus

$$P(\text{Resp} | \text{Stim}, \text{PA}) = \frac{P(\text{PA} | \text{Stim}, \text{Resp}) * P(\text{Resp} | \text{Stim})}{P(\text{PA} | \text{Stim})} \quad (4)$$

where Resp is behavioral outcome, Stim is stimulus identity (S+ or S-), and PA is baseline pupil size. For computing probabilities based on baseline pupil size, the baseline range of each session was first computed and then evenly broken into 20 bins, into which single trial baseline pupil areas could be sorted.

Leave-one-out-cross-validation (LOOCV) on each session was used to test the performance of the predictor (Bishop 2006). The likelihood and prior probabilities were computed from training data from one session. The behavioral output was then predicted for the left-out trial. After repeating this for every trial, the probability of correct predictions was calculated for each session individually.

Regression Analysis

To quantitatively confirm the linear and/or quadratic relationship between pupil baseline and HR, FAR, d' , and decision criterion, we performed a regression analysis to evaluate the weights of the linear and quadratic components of each relationship (van den Brink et al. 2016). For each session, a polynomial of degree 2 was fit using least-squares to the relationship between HR, FAR, d' , and decision criterion vs. pupil baseline. The first- and second-degree components were reported, and the Wilcoxon signed-rank test was used to determine whether each relationship exhibited a significant linear and/or quadratic relationship.

Statistics

To compare multiple group distributions, one-way ANOVA tests were performed. Post hoc Tukey's honest significance difference (HSD) test was performed for all multiple comparisons. Prior to all other statistical tests, the one-sample Kolmogorov-Smirnov test was used to assess the normality of the data. If the samples were normally distributed, a Student's t -test was used. Otherwise, the Mann-Whitney U -test was used for unpaired samples or the Wilcoxon signed-rank test for paired samples. Bonferroni correction was implemented for multiple comparisons.

RESULTS

Behavioral Performance in a Whisker Deflection Direction Discrimination Task

To understand pupil dynamics during behavior, we trained five head-fixed rats to perform a Go/No-Go tactile discrimination task. A head-restrained paradigm allowed us to precisely deliver tactile stimuli via a computer-controlled piezoelectric actuator to animals performing the task while their pupil was imaged (Fig. 1A). Tactile stimuli were single whisker deflections with half-sinusoidal waveforms (15° of deflection, 3 durations: 25, 50, and 100 ms; 2 directions: dorsal or ventral). These three stimulus durations correspond to the mean whisker deflection velocities of 1,200, 600, and 300°/s, respectively. With the use of the Go/No-Go discrimination paradigm, whisker deflections to the dorsal direction were randomly designated as Go stimuli (S+ stimuli), whereas whisker deflections to the ventral direction were designated as No-Go stimuli (S- stimuli) for all animals used in this study (Fig. 1B). Following stimulus presentation, the animals decided whether to respond by licking or withholding a response within a 1.3-s window of opportunity initiated at stimulus onset, yielding four possible behavioral outcomes: hit (i.e., licking in response to S+ stimuli), CR (i.e., no licking following S- stimuli), FA (i.e., licking in response to S- stimuli), and miss (i.e., no licking in response to S+ stimuli) (Fig. 1B). After becoming experts (see MATERIALS AND METHODS), the animals were proficient in discriminating between the directions of whisker deflections, evidenced by significantly more responses to S+ than to S- stimuli (Fig. 1C). In this study, we only analyzed data from sessions in which pupillometry was taken. For these sessions, the HR was significantly higher than FAR (0.754 ± 0.163 vs. 0.362 ± 0.181 , $P < 1.0 \times 10^{-19}$, Wilcoxon signed-rank test, Fig. 1, D and E).

Using signal detection theory, we first examined the effect of stimulus waveform durations on perceptual sensitivity and decision criterion. The six stimuli (3 S+ stimuli, i.e., dorsal whisker deflection with 3 durations, and 3 S- stimuli, i.e., ventral whisker deflection with 3 durations) were presented during the discrimination task in a random fashion with equal probabilities. Perceptual sensitivity (d') varied across these stimulus waveform durations [Fig. 1F; $P < 6.4 \times 10^{-8}$, $F(2, 329) = 17.44$, one-way ANOVA test]; specifically animals were less sensitive in discriminating between deflections with shorter durations. Tukey's HSD post hoc test revealed that d' was significantly smaller for durations of 25 ms than durations of 50 ms (0.833 ± 0.630 vs. 1.290 ± 0.720 , $P < 7.0 \times 10^{-6}$) or durations of 100 ms (1.360 ± 0.790 , $P < 1.6 \times 10^{-7}$) but did not differ between durations of 50 ms and 100 ms ($P = 0.76$) (Fig. 1F). Intriguingly, the duration of the stimulus waveform had a significant effect on the animals' decision criterion (i.e., decision bias) [$P < 0.003$, $F(2, 329) = 6.03$, 1-way ANOVA test], as the animals became more liberal when discriminating between the stimuli with the shortest (criterion = -0.352 ± 0.650) and longest durations (criterion = -0.102 ± 0.430 ; $P < 0.0017$, Tukey's HSD post hoc test). The decision bias of the middle duration stimulus did not significantly differ from either the shortest or longest (criterion = -0.259 ± 0.048 ; $P = 0.3749$ and $P = 0.086$, respectively, Tukey's HSD post hoc test). The duration of the stimulus waveform did not appear to affect reaction times [Fig. 1G; 0.589 ± 0.120 s for 25

ms vs. 0.592 ± 0.110 s for 50 ms vs. 0.602 ± 0.110 s for 100 ms, $P = 0.69$, $F(2, 329) = 0.37$, 1-way ANOVA test], suggesting that stimulus intensity was sufficiently high.

To examine whether the time elapsed between trial onset and stimulus presentation affected the animals' behavioral performance, we calculated HR and FAR for trials with short delays (duration between trial onset and stimulus presentation was shorter than the mean delay, i.e., 2.25 s, see MATERIALS AND METHODS) and long delays (delay was greater than the mean delay). Short delays did not result in different HRs (Fig. 1H; 0.746 ± 0.170 s for short delay vs. 0.753 ± 0.170 s for long delay, $P = 0.33$, Wilcoxon signed-rank test), FARs (0.350 ± 0.200 s for short delay vs. 0.353 ± 0.180 s for long delay, $P = 0.60$, Wilcoxon signed-rank test), perceptual sensitivity (1.198 ± 0.740 for short delay vs. 1.228 ± 0.670 for long delay, $P = 0.71$, Wilcoxon signed-rank test), or decision criterion than longer delays (-0.167 ± 0.480 short delay vs. -0.194 ± 0.470 for long delay, $P = 0.12$, Wilcoxon signed-rank test). Moreover, the duration between trial onset and stimulus did not have any effects on reaction time [Fig. 1I; $P = 0.99$, $F(24, 2669) = 0.42$, 1-way ANOVA test], suggesting that this short waiting period before stimulus presentation did not affect the behavioral state that influences perceptual performance of the animals (Moradi et al. 2007).

Four Behavioral Outcomes Were Associated with Different Pupil Dynamics

To examine the extent to which fluctuations in pupil size correlate with behavioral performance during this tactile discrimination task, we imaged the left eye of the animals at 10 Hz throughout the task. Pupil size was then estimated offline by automatically segmenting the pupil from images (Fig. 2A) (Liu et al. 2017). We found that the pupil dilated following stimulus presentation on each trial. However, pupil dynamics varied both preceding and following stimulus presentation for the four behavioral outcomes (Fig. 2B). For hit, CR, and miss trials, pupil dilations exhibited biexponential curve shapes, similar to the pupil dilation elicited by phasic locus coeruleus (LC) activation (Joshi et al. 2016; Liu et al. 2017). However, in FA trials, the dilations plateaued, and the pupil size remained constant for several seconds.

Pupil baseline, measured as the mean Z-scored pupil size during the 0.5 s preceding stimulus presentation, varied across the four response outcomes [Fig. 2C; $P < 5.3 \times 10^{-7}$, $F(3, 437) = 11.04$, 1-way ANOVA test]. Specifically, average baseline pupil size was larger for FA trials than miss and CR trials (-0.102 ± 0.240 for FA trials vs. -0.252 ± 0.320 for miss trials vs. -0.236 ± 0.210 for CR trials, $P < 2.8 \times 10^{-5}$, and $P < 2.2 \times 10^{-4}$, respectively, Tukey's post hoc test), whereas there was no significant difference between FA and hit trials (-0.123 ± 0.170 for hit trials, $P = 0.92$, Tukey's post hoc test). Moreover, pupil baseline of hit trials was also significantly larger than miss and CR trials ($P < 4.7 \times 10^{-4}$, and $P < 0.003$, respectively, Tukey's post hoc test), whereas there was no significant difference between miss and CR baselines ($P = 0.96$, Tukey's post hoc test). Consequently, pupil baseline in trials when the rats responded was significantly larger than in trials when they withheld a response (responded: -0.121 ± 0.170 , withheld: -0.230 ± 0.180 , $P < 3.6 \times 10^{-6}$, Wilcoxon signed-rank test).

To quantitatively examine the correlation between pupil baseline and behavior, we used MAP estimations to predict behavioral outcomes from pupil baseline before stimulus delivery. When based solely on pupil baseline before stimulus delivery, we calculated the posterior probability distribution of $P(\text{behavioral response} \mid \text{pupil baseline})$ from estimated prior $P(\text{behavioral response})$ and likelihood $P(\text{pupil baseline} \mid \text{behavioral response})$. The posterior distribution model was built using data from all trials except a randomly selected trial (i.e., test trial). We then used this model to predict the behavioral outcome of the test trial from its pupil baseline. This LOOCV was repeated until all trials were used as a test trial. We found this estimation correctly predicted behavioral outcome in $41.2 \pm 8.2\%$ of trials, which is significantly greater than a chance level (i.e., 25% chance of any of the 4 unique outcomes), by $16.22 \pm 8.20\%$ (Fig. 2D). When incorporating the knowledge of stimulus identity into the model, this model predicted whether the animal would respond and had $73.6 \pm 9.5\%$ chance to correctly predict behavior, an $\sim 23\%$ increase from the chance level (i.e., 50% chance of whether a response was made or not) (Fig. 2D). Intriguingly, the performance of this pupil-baseline-based Bayesian decoder was related to perceptual performance, as the probability of correct predictions in a session was positively correlated with the

perceptual sensitivity of that session (Fig. 2E; $P < 3.48e-12$), suggesting that pupil baseline was strongly correlated with perceptual processing. There were also negative linear correlations between both mean pupil baseline (Fig. 2F, $P < 3.67e-3$) and within-session variance in pupil baseline (Fig. 2G, $P < 4.04e-3$) vs. perceptual sensitivity, indicating that animals maintained better sensitivity in sessions with overall lower and less variable pupil-linked arousal.

Similarly, pupil dilations, measured as the difference between the greatest value that the pupil size reached within 4.5 s following stimulus presentation and the pupil baseline, were significantly different in trials with different behavioral outcomes [Fig. 3A; $P < 1.7e-50$, $F(3, 437) = 103.38$, 1-way ANOVA test]. Following either an S+ or S- stimulus, the dilations were much larger in trials in which the animals responded (responded: 0.69 ± 0.40 vs. withheld: 0.11 ± 0.12 , $P < 3.7e-19$, Wilcoxon signed-rank test), likely attributable to pupil dilation associated with motor activities (Lee and Margolis 2016). Interestingly, even for trials in which the animal responded, dilations during hit trials were larger than in FA trials (0.832 ± 0.470 for hit trials vs. 0.489 ± 0.320 for FA trials, $P < 3.8e-9$, Tukey's post hoc test), suggesting that rewards and punishment (i.e., timeout period) may result in different pupil dilation profiles. Interestingly, for trials in

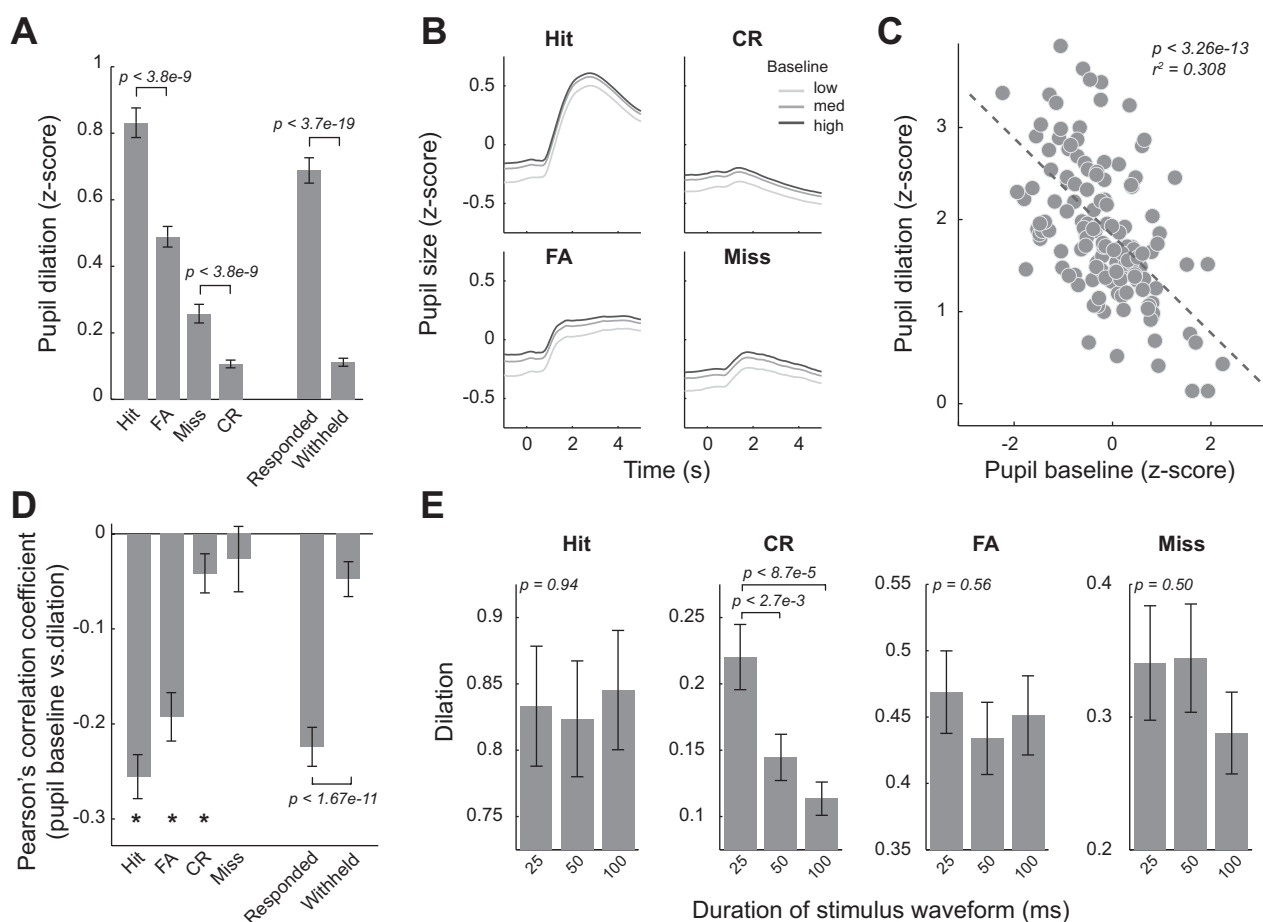


Fig. 3. Pupil dilation was inversely correlated with pupil baseline. **A**: pupil dilations for the 4 behavioral outcomes averaged across sessions. **B**: pupil dynamics around stimulus presentation plotted with low, medium, and high pupil baselines, averaged across all sessions of the 5 animals. **C**: example scatter plot showing a negative correlation between pupil baseline and dilation for hit trials. Each dot represents a trial. **D**: there was a significantly negative correlation between pupil baseline size and pupil dilation on single-trial basis for hit, false alarm (FA), and correct rejection (CR) behavioral outcomes. **E**: dilations as a function of stimulus waveform duration for all behavioral outcomes. Only in CR trials, stimulus waveform duration affected pupil dilation. Error bars indicate SE; * $P < 0.01$.

which the animal did not respond, miss trials were associated with larger pupil dilation than CR trials (0.258 ± 0.290 for miss trials vs. 0.107 ± 0.120 for CR trials, $P < 3.8 \times 10^{-9}$, Tukey's HSD post hoc test).

Pupil Baseline Was Inversely Correlated with Pupil Dilation

Although the pupil dilated in each response outcome, it was unclear whether pupil baseline had effects on subsequent pupil dilation. To test this, for each response outcome, we categorized pupil baseline into three groups: low (<33% maximum baseline), medium (33% and <66% maximum baseline), and high (>66% maximum baseline) and plotted pupil dynamics for each group (Fig. 3B). Consistent with previous work (Murphy et al. 2011), it was qualitatively evident that the amplitude of pupil dilation was greater when pupil baseline was smaller. The smaller pupil dilation associated with larger pupil baseline was not likely because pupil size reached its physical limit because pupil dilation in FA and CR trials was significantly smaller than in hit trials, but pupil baseline was still inversely correlated with pupil dilation for these behavioral outcomes. This trend also holds on a trial-by-trial basis (Fig. 3C). To quantify this inverse correlation, we calculated Pearson's correlation coefficient between pupil baseline and dilation on a single trial basis and found significant correlation for all response types except miss responses (Fig. 3D; Hit: $P < 1.7 \times 10^{-14}$; FA: $P < 5.9 \times 10^{-10}$; CR: $P < 0.003$; Miss: $P = 0.175$, Wilcoxon signed-rank test). Moreover, the correlation was greater in responded than withheld trials ($P < 4.7 \times 10^{-11}$, Wilcoxon signed-rank test).

Although stimulus waveform duration affected perceptual sensitivity and decision criterion, it did not affect the dilation in hit trials [Fig. 3E; $P = 0.94$, $F(2, 329) = 0.06$, 1-way ANOVA test]. This is probably because, in addition to sensory processing and decision making, other processes, such as motor activity (i.e., licking) and reward, also resulted in pupil dilation (Lee and Margolis 2016). Indeed, when quantifying pupil dilation in response to stimuli with the three durations in CR trials, in which neither motor activity nor feedback occurred, we found stimulus duration had a significant effect on pupil dilation [$P < 8.0 \times 10^{-5}$, $F(2, 320) = 9.71$, 1-way ANOVA]. Pupil dilation in response to stimuli with 25-ms durations was significantly larger than stimuli with durations of either 50 or 100 ms ($P < 2.7 \times 10^{-3}$, and $P < 8.7 \times 10^{-5}$, respectively, Tukey's HSD test), whereas the dilations between 50- and 100-ms stimulus durations did not differ ($P = 0.66$, Tukey's HSD post hoc test). It is interesting to note that perceptual sensitivity to stimuli with 25-ms durations was also significantly lower than for the other durations (Fig. 1F).

Pupil Baseline Exhibited an Inverted U-Shaped Relationship with Perceptual Sensitivity and a U-Shaped Relationship with Decision Criterion

While animals performed, the pupil size of the animals rapidly fluctuated throughout the task despite constant ambient illuminance (Fig. 4, A and F, for population data). In addition, HR and FAR rapidly changed across trials (Fig. 4B), resulting in fluctuations in perceptual sensitivity (Fig. 4C) and decision criterion (Fig. 4D). Furthermore, reaction times for both correct trials (hits) and incorrect trials (FAs) varied across trials (Fig. 4E). Correlation analysis revealed that there was no

significant linear correlation between baseline pupil size and perceptual sensitivity or decision criterion, as their Pearson's correlation coefficients did not deviate from 0 (Fig. 5A; $P = > 0.20$, and $P = 0.20$, respectively, Wilcoxon signed-rank test). However, across all trials, we found that pupil dilation following stimulus presentation was linearly correlated with decision criterion ($P < 1.4 \times 10^{-9}$, Wilcoxon signed-rank test) but not perceptual sensitivity ($P = 0.08$, Wilcoxon signed-rank test). This relationship between dilation and criterion may be explained by the large dilations associated with hit and FA trials, in which the animals were likely to have highly liberal criteria (i.e., more negative decision criteria).

Although Pearson's correlation coefficients between pupil baseline and perceptual sensitivity/decision criterion were not significantly different from 0, it did not rule out the possibility that there was a nonlinear correlation between them. To further examine their relationship, we divided pupil baselines into 20 groups and calculated the percentage of trials in which the pupil baseline was within each group. Although the pupil was occasionally largely dilated in some trials, in the majority of trials (>60% of trials), pupil baseline was within 10–40% of maximum pupil baseline (Fig. 5B). We then calculated the average HR and FAR for each of these 20 bins. We found that pupil baseline exhibited an inverted U-shaped relationship with HR (Fig. 5C). Moreover, FAR increased linearly with size of pupil baseline, resulting in an inverted U-shaped relationship between pupil baseline and perceptual sensitivity (Fig. 5D) and a U-shaped relationship between pupil baseline and decision criterion (Fig. 5E). Regression analysis (see MATERIALS AND METHODS) confirmed that HR, d' , and decision criterion had quadratic relationships with pupil baseline (Fig. 5F; $P < 2.5 \times 10^{-9}$ for HR; $P < 4.5 \times 10^{-4}$ for d' ; $P < 4.6 \times 10^{-7}$ for criterion, Wilcoxon signed-rank test), whereas FAR only had a linear relationship with pupil baseline ($P < 1.1 \times 10^{-3}$ for linear component; $P = > 0.348$ for quadratic component, Wilcoxon signed-rank test). Intriguingly, decision criterion also had a significant negative relationship with pupil baseline ($P < 8.8 \times 10^{-6}$, Wilcoxon signed-rank test).

Shorter Reaction Time Was Associated with Higher Perceptual Sensitivity, More Liberal Decision Criterion, and Larger Pupil Baseline

Previous studies suggested a correlation between reaction times and behavioral states (Mauri et al. 2015; Moradi et al. 2007). In this light, we examined the relationship between reaction times of the animals with their behavioral performance and pupil dynamics by calculating HR/FAR and average reaction time using a 30-trial sliding window. The average reaction time was used to map perceptual sensitivity/decision criterion to percentage of maximum normalized reaction time of the session (see MATERIALS AND METHODS). We found that both HR and FAR decreased as reaction time increased (Fig. 6A). However, HR decreased at a faster rate than FAR. Consequently, when calculated using a 30-trial sliding window, perceptual sensitivity also decreased with the increase of reaction times (Fig. 6B; $P < 3.09 \times 10^{-7}$). Interestingly, animals were also more conservative in trials with longer reaction times, evidenced by an increase in decision criterion along with increase in reaction time (Fig. 6C; $P < 4.91 \times 10^{-11}$).

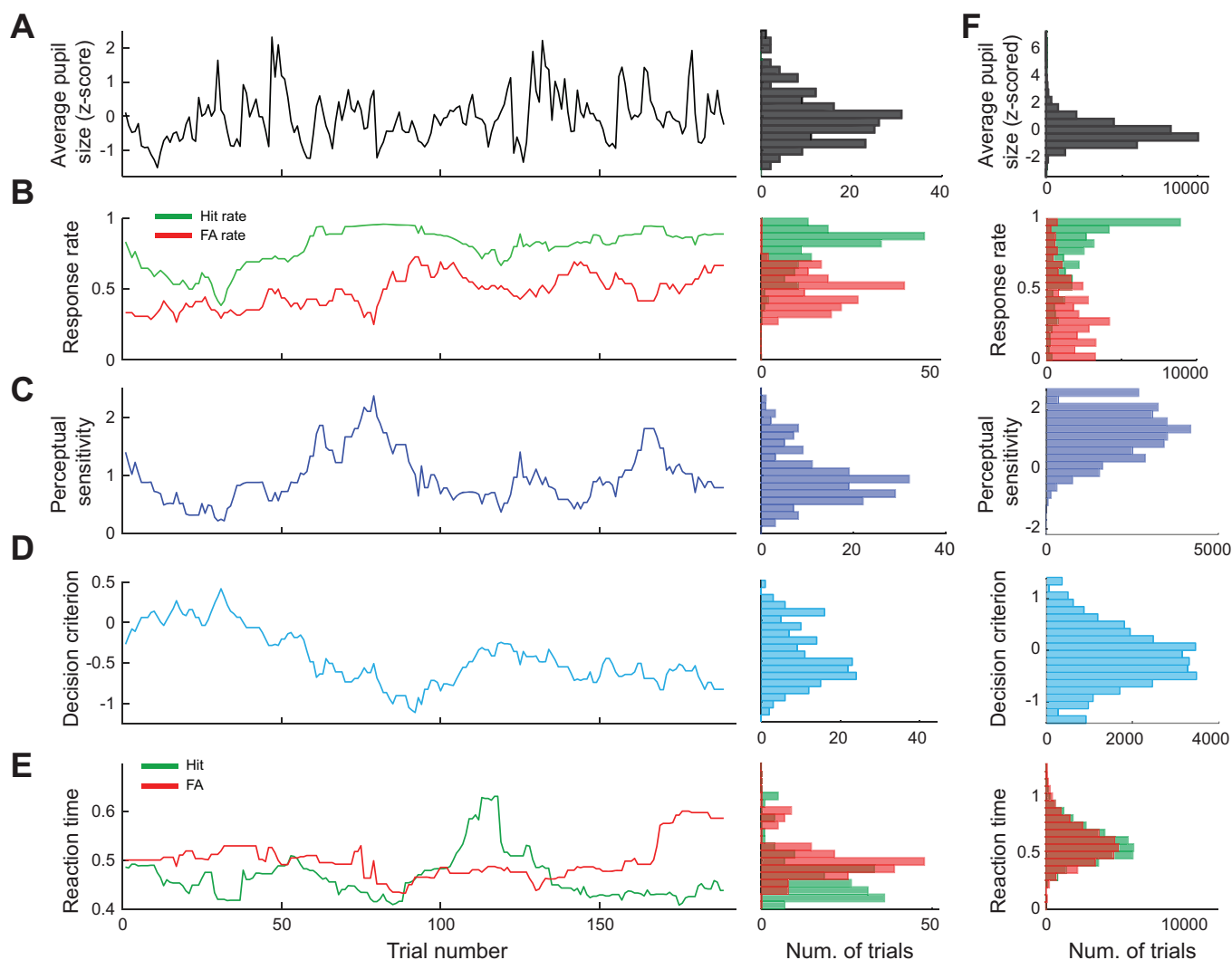


Fig. 4. Pupil size, behavioral performance, and reaction time fluctuated throughout behavioral tasks. Example session showing fluctuation of pupil baseline area (A), hit and false alarm (FA) rates (B), perceptual sensitivity (C), decision criterion (D), and reaction time (E). Distribution of population data across all sessions is shown (F). Data are calculated across 30 trial windows.

We next tested whether changes in reaction times were associated with fluctuations of pupil dynamics. Similarly, we plotted reaction time vs. pupil baseline, both in percentage of maximum value of each session, for all responded trials in which a reaction time was logged (i.e., hit and FA trials). Because pupil baseline in the majority of trials was between 10 and 40% of maximum pupil baseline, the average pupil baseline for each reaction time bin was around 30% of maximum pupil baseline. However, pupil baseline exhibited a descending trend with reaction time (Fig. 6D, $P = 0.036$ and $r^2 = 0.177$). To further characterize the relation between reaction times and pupil dynamics, we divided all hit and FA trials into a slow reaction group (reaction time $>$ mean reaction time) and fast reaction group (reaction time $<$ mean reaction time; see MATERIALS AND METHODS) and plotted pupil dynamics around stimulus presentation for both slow and fast reaction groups (Fig. 6, E and G). As we expected, for both hit and FA trials, pupil baseline of the slow reaction group was significantly smaller than the fast reaction group (Fig. 6, F and H; $P < 0.04$ for hit trials, and $P < 0.04$ for FA trials, Wilcoxon signed-rank test). Also, pupil dilation following stimulus presentation was

significantly bigger for the slow reaction trials than the fast reaction trials (Fig. 6, F and H; $P < 2.7e-11$ for hit trials, and $P < 2.5e-7$ for FA trials, Wilcoxon signed-rank test).

Behavioral Outcome Influenced Upcoming Pupil Dynamics and Behavior

As Fig. 4 illustrates, behavioral performance and pupil dynamics fluctuated throughout sessions for all animals in this study. We hypothesized that the fluctuation of behavioral performance was primarily due to fluctuations of behavioral state. To test this, we first plotted pupil dynamics aligned by stimulus presentation for the four behavioral outcomes conditioned upon previous outcomes (Fig. 7A). Interestingly, pupil baseline following hit trials was significantly larger than average pupil baseline (Fig. 7B; $P < 9.77e-13$, Wilcoxon signed-rank test), whereas pupil baselines following other behavioral outcomes were smaller than average baseline (after CR: $P < 2.5e-18$; after FA: $P < 1.4e-4$; after miss: $P < 2.8e-10$; Wilcoxon signed-rank test). In addition to this relationship with pupil baseline, the behavior outcome of the previous trial

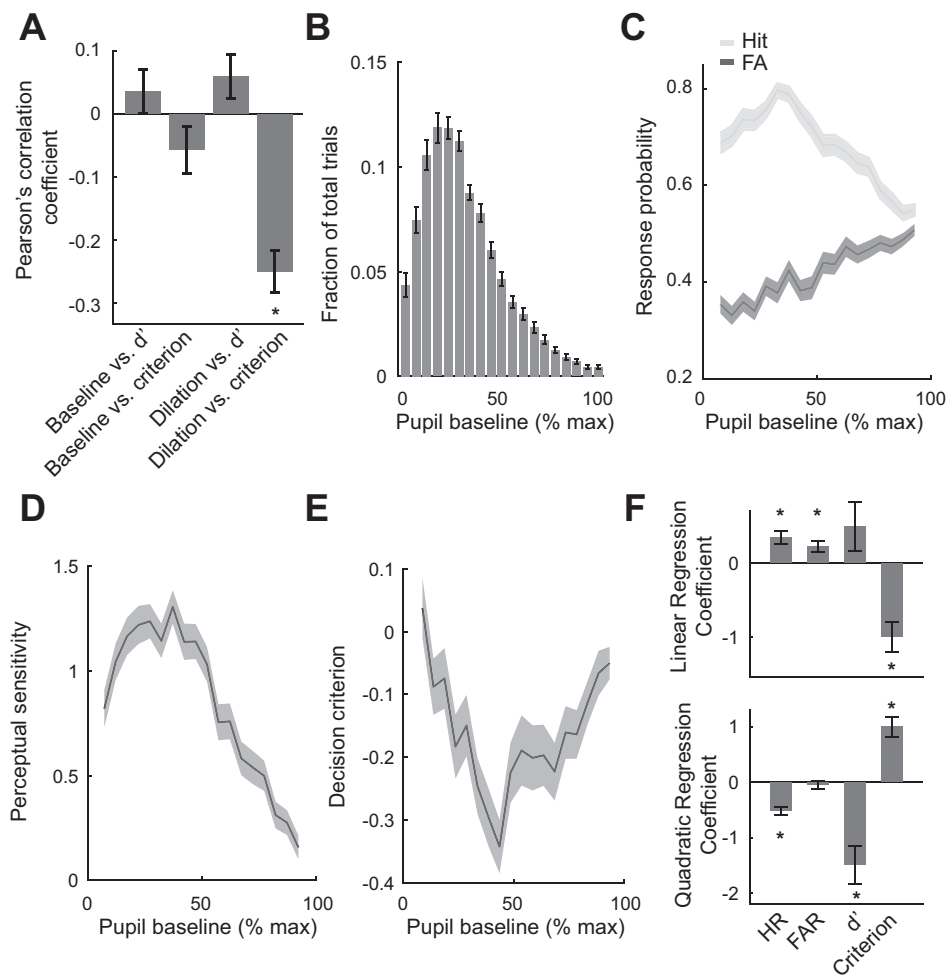


Fig. 5. Pupil baseline exhibited an inverted U-shaped relationship with perceptual sensitivity and U-shaped relationship with decision criterion. *A*: there was no significant linear relationship between pupil baseline and perceptual sensitivity/decision criterion. Pupil dilation in response to stimulus was linearly correlated with decision criterion but not perceptual sensitivity. *B*: pupil baseline was within 10–40% of maximum pupil baseline for the majority of trials. *C*: relationship between pupil baseline and hit rates (HR) as well as false alarm rates (FAR). *D*: pupil baseline exhibited an inverted U-shaped relationship with perceptual sensitivity. *E*: pupil baseline exhibited a U-shaped relationship with decision criterion. *F*: regression coefficients of HR, FAR, perceptual sensitivity (d'), and criterion curve with regard to pupil baseline. Error bars and shaded areas indicate SE; $*P < 0.05$.

was also correlated with the behavior outcome of the present trial. HR and FAR on trials following hit trials were significantly higher than average (Fig. 7C; $P < 8.2e-15$ for HR, and $P < 1.3e-17$ for FAR, Wilcoxon signed-rank test). Similarly, HR on trials following CR responses was higher than average ($P < 2.6e-6$, Wilcoxon signed-rank test). However, unlike trials following hit trials, FAR following CR trials was lower than average ($P < 2.0e-9$, Wilcoxon signed-rank test), resulting in a significantly larger perceptual sensitivity following CR trials compared with the session average d' (i.e., average d' across sessions) (Fig. 7D; $P < 3.4e-12$; Wilcoxon signed-rank test).

Although, in general, animals were liberal in the discrimination task, as evidenced by a negative average decision criterion, following hit trials, animals became even more liberal; decision criteria for trials following hits were significantly smaller than the session average (Fig. 7E; -0.610 ± 0.600 vs. -0.210 ± 0.450 , respectively, $P < 9.6e-18$, Wilcoxon signed-rank test). However, decision criteria for trials following CR and FA were closer to neutral (i.e., criterion = 0) (-0.107 ± 0.440 and 0.045 ± 0.680 for following CR and FA trials, respectively), whereas those following miss trials were more conservative (0.481 ± 0.350), indicating that the dependence of behavior on the outcome of the previous trial was primarily due to fluctuation of behavioral state. This suggests that pupil-linked arousal modulates perceptual performance

because, if the animals were adaptively adjusting their behavior in response to the previous behavioral outcome, one would instead expect them to raise their decision criterion after an FA, lower their decision criterion after a miss, and not change anything after a CR.

In further support of this notion, reaction time was significantly faster than average following hit trials (Fig. 7F; 0.568 ± 0.110 vs. 0.595 ± 0.110 , $P < 2.4e-11$, Wilcoxon signed-rank test), whereas it was significantly slower for trials following other behavioral outcomes (0.630 ± 0.120 s for following CR, 0.619 ± 0.130 s for following FA, and 0.619 ± 0.130 s for following miss; $P < 1.6e-10$, $P < 1.6e-5$, and $P < 1.4e-4$, respectively, Wilcoxon signed-rank test).

DISCUSSION

The present study was designed to allow us to investigate 1) whether head-fixed rats are able to discriminate between different directions of passive whisker movement, 2) the correlation between pupil dynamics, perceptual performance, and reaction time in rats performing a perceptual discrimination task, and 3) to what extent pupil size before stimulus is predictive of behavior in the discrimination task. Rats have proven to be capable of various tactile tasks, including detection of whisker stimulation and discrimination between different object locations and shapes (Brecht et al. 1997; O'Connor

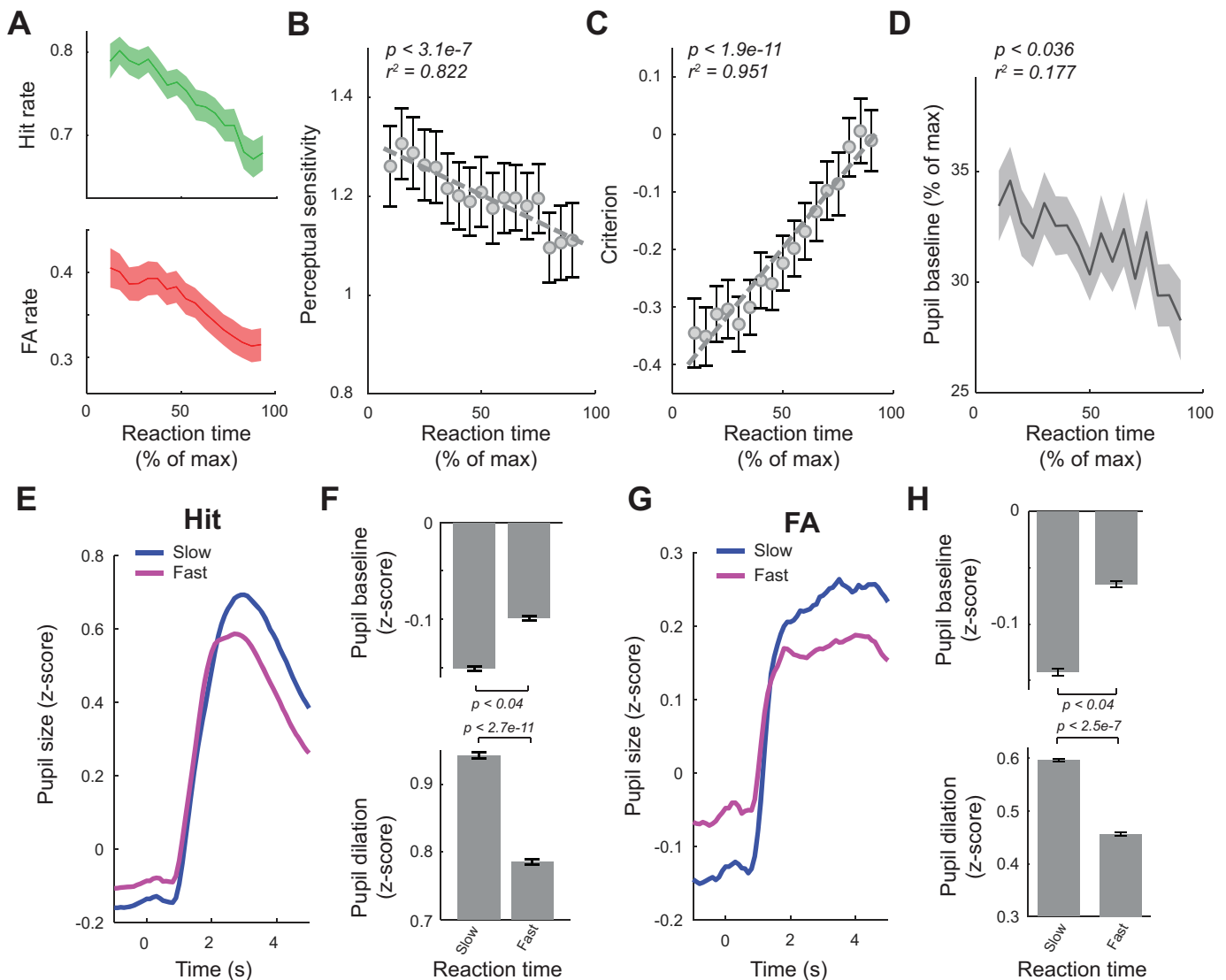


Fig. 6. Reaction time was correlated with behavioral performance and pupil dynamics. *A*: both hit and false alarm (FA) rates decreased as reaction time increased. *B*: perceptual sensitivity decreased as reaction time increased. *C*: decision criterion increased with reaction time. *D*: pupil baseline exhibited a weak negative correlation with reaction time. *E* and *F*: pupil dynamics in slow vs. fast trials for hit trials. *G* and *H*: pupil dynamics in slow vs. fast trials for FA trials. Error bars and shaded areas indicate SE.

et al. 2010a; O'Connor et al. 2010b), whisker vibrations (Adibi et al. 2012; Gerdjikov et al. 2010), textures (Carvell and Simons 1990; Ritt et al. 2008; von Heimendahl et al. 2007), and aperture widths (Krupa et al. 2004). Here, we showed that rats were also able to discriminate between different directions of whisker deflections. The minimal velocity of whisker deflection used in the study was ~ 300 %/s, which was above detection threshold measured using a similar setup (Ollershaw et al. 2012; Stüttgen and Schwarz 2008). Interestingly, the average reaction time of our tactile discrimination tasks was substantially longer than those reported in rats performing the tactile detection tasks (Ollershaw et al. 2012; Stüttgen and Schwarz 2008). This suggests that additional mental effort may be exerted when discriminating between different tactile stimuli compared with only detecting the presence of a tactile stimulus.

Discrimination performance deteriorated as stimulus duration decreased and thus as mean stimulus velocity increased

because the velocity varied with the stimulus duration, given the fixed stimulus amplitude in our study. This decrease in discrimination performance may be due to the reduction in time for the animal to accumulate evidence concerning the direction of the whisker deflection to make Go or No-Go decisions (Gold and Shadlen 2007). Neurons in the thalamus and cortex of the whisker pathway display strong sensitivity to the velocity of whisker movement; thus another explanation is that the velocity of the shortest duration stimulus was too strong and saturated the neural responses within the pathway, leading to deterioration in performance (Lee and Simons 2004; Millard et al. 2013; Pinto et al. 2000; Stüttgen and Schwarz 2008; Zheng et al. 2015). However, the peak velocity of whisker movement associated with stick-slip events (repeated sticking then high-acceleration slipping over surfaces when rats whisk across objects) is comparable to the highest velocity used in this study (i.e., $\sim 1,200$ %/s) (Jadhav et al. 2009; Ritt et al. 2008). Future work is warranted to decouple the effect of

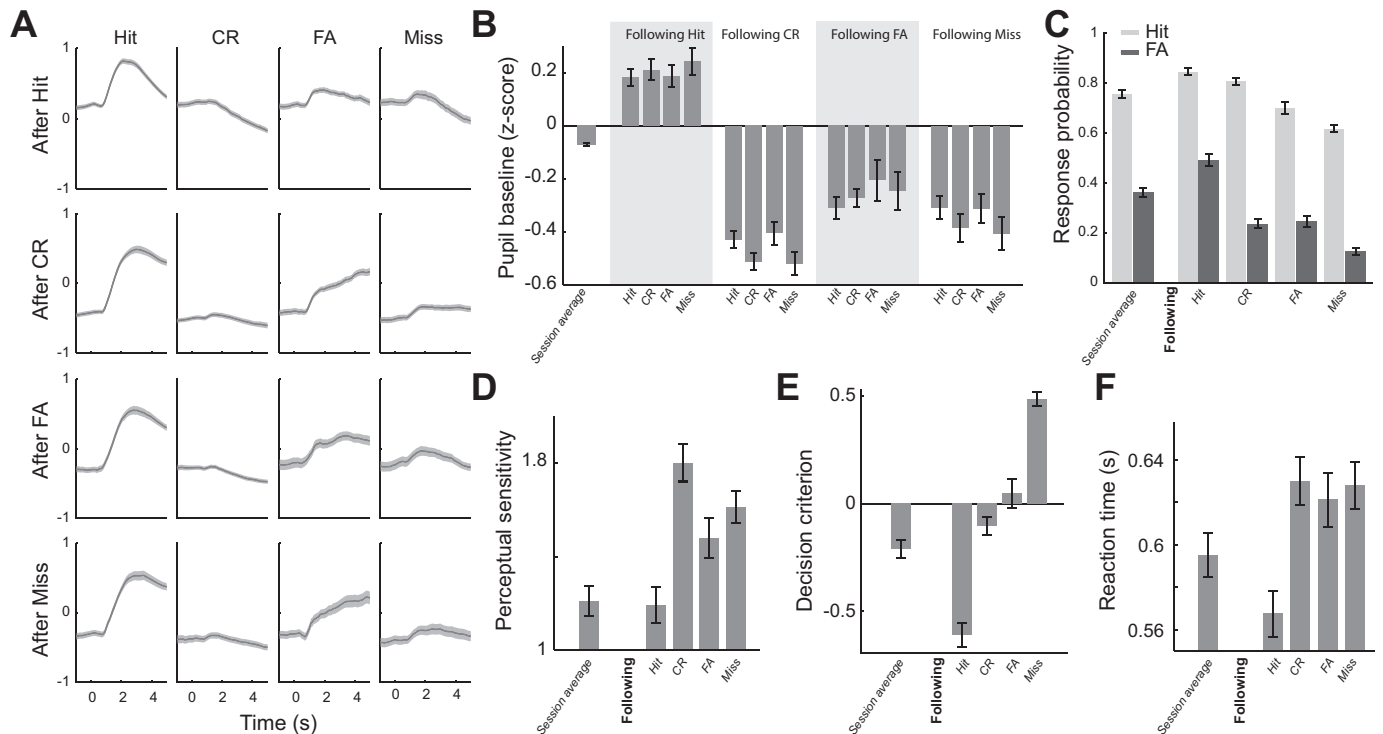


Fig. 7. Behavioral outcomes of the previous trial influenced pupil dynamics and behavior in the present trial. *A*: pupil responses conditioned on previous response, averaged across sessions. *B*: pupil baseline of the 4 behavioral outcomes conditioned on the previous response. *C*: hit and false alarm (FA) rates conditioned on the previous response. *D*: perceptual sensitivity conditioned on the previous response. *E*: decision criterion conditioned on the previous response. *F*: reaction times conditioned on the previous response. Error bars and shaded areas indicate SE. CR, correct rejection.

stimulus duration and stimulus velocity in whisker deflection direction discrimination task.

In this study, all behavioral tasks were performed in the light phase. Although rats are naturally nocturnal and tend to be more active during dark phases, it remains controversial whether to perform behavioral tasks for rodents strictly in their dark phases (Adibi et al. 2012; Roedel et al. 2006; Yang et al. 2008). Our data showed that the animals performed sufficiently well in the discrimination tasks, presumably attributable to their strong desire for rewards, the fact that the tasks were performed inside a light attenuation chamber, or both. However, it remains possible that their behavioral performance might not be optimal in the light phase. Although this study focuses on how fluctuating pupil-linked arousal relates to behavior, a future study to systematically compare the effects of light and dark phase on performance of the tactile discrimination task would be intriguing.

In the Go/No-Go paradigm, we found the pupil dilated following stimulus presentation for all behavioral outcomes. In response trials, pupil dilation was larger compared with withhold trials. Additionally, although hit trials exhibited biexponential curve shapes, FA trials exhibited a smaller but sustained dilation, possibly attributable to anticipation of a time-out period indicated by a prolonged timeout tone. The largest pupil dilations associated with hit trials are likely due to motor activity and reward, as Lee and Margolis (2016) found that licking to random water rewards resulted in pupil dilation. Consistent with this notion, movement was previously reported to associate with pupil dilation (McGinley et al. 2015a; Musall et al. In press; Reimer et al. 2014; Stringer et al. In press; Vinck et al. 2015). It is important to note that, in CR and miss trials,

there was neither feedback nor obvious motor activity related to licking. Therefore, the pupil dilation likely resulted solely from internal task-related cognitive processing. It is intriguing that pupil dilations in miss trials were greater than CR trials. In other words, dilation induced by incorrect information processing was larger than from correct information processing, suggesting that more mental efforts were exerted in trials with more internal noise and possibly uncertainty about stimulus identity (Yu and Dayan 2005) or error detection (Yeung et al. 2004) (also see discussion below). In support of this notion, we found that, in CR trials, animals' pupils dilated more when discriminating harder stimuli (Fig. 3E). This is consistent with previous work, in which human subjects' pupils dilated more when solving more difficult math problems, arguably due to increased mental load (Hess and Polt 1964).

Behavioral performance is heavily dependent on arousal (Aston-Jones and Cohen 2005; McGinley et al. 2015b; Wexselblatt and Niell 2015; Yerkes and Dodson 1908). Several studies have attempted to map pupil-linked arousal to animal behavioral performance (Lee and Margolis 2016; McGinley et al. 2015a). For example, it was found that mice performing a detection task had optimal performance, while pupil-linked arousal was intermediate, exhibiting an inverted U-shaped curve depicted by the Yerkes-Dodson law (McGinley et al. 2015a). Similarly, we found that our animals had peak perceptual sensitivity in discriminating different directions of whisker movement when their pupil baseline was ~40% of the maximal pupil baseline size. In addition to a quadratic relationship, we found a negative linear relationship between pupil baseline and decision criterion, which is in line with recent work in humans

that attributed this to pupil indexed modulation of global neural gain (Murphy et al. 2016).

Non-luminance-mediated pupil dilation in behavior has long been hypothesized to result from activation of the LC, a brain structure involved in regulation of arousal and the primary source of norepinephrine to the forebrain (Aston-Jones and Cohen 2005; Carter et al. 2010; Sara 2009). In monkeys performing Go/No-Go visual detection tasks, LC neurons responded phasically to Go stimuli, whereas the responses to No-Go stimuli that produced CRs were much weaker and were followed by an inhibition (Rajkowski et al. 2004). In line with these findings, the pupil dilation of our animals in hit trials had a similar biexponential shape to that evoked by phasic LC stimulation. Interestingly, pupil dilation in CR trials was significantly smaller than that in hit trials and was also followed by constriction (Fig. 2B).

In awake animals, extracellular recordings in the LC showed that LC firing rate covaried with pupil size (Aston-Jones and Cohen 2005; Joshi et al. 2016). In humans, fMRI studies suggested a positive correlation between blood oxygen level-dependent signal in LC and pupil size (de Gee et al. 2017; Murphy et al. 2014). Several recent animal studies demonstrated the causal relationship between LC activation and pupil dilation, with brief phasic LC activations evoking large transient pupil dilations, whereas low-frequency tonic LC activation gradually dilated the pupil (Joshi et al. 2016; Liu et al. 2017; Reimer et al. 2016). Moreover, the LC activation-mediated pupil dilation is through LC control of both sympathetic and parasympathetic systems, whereas the parasympathetic contribution is significantly larger than the sympathetic contribution (Liu et al. 2017). Our data showed that the pupil of behaving rats started to dilate ~900 ms following the presentation of the sensory stimulus (Fig. 2B). This lag is consistent with the lag between pupil dilation and phasic electrical microstimulation of the LC in rodents (Liu et al. 2017).

In monkeys performing Go/No-Go detection tasks, LC responses to sensory stimuli in miss and CR trials were comparable (Rajkowski et al. 2004). However, our data showed that pupil dilation in miss trials was significantly larger than that in CR trials. This discrepancy may be due to inherent differences between the detection and discrimination paradigms. Given the generally liberal decision criterion we observed, it may take more effort for the animals to refrain from responding in the presence of a Go stimulus. However, it is noteworthy that a recent work found that, in addition to the LC, the activity of several other brain structures, including the inferior colliculus (IC), the intermediate layer of the superior colliculus (SCi), and the anterior cingulate cortex (ACC), also covaried with pupil size (Joshi et al. 2016). Because the LC sends dense projections to virtually the entire forebrain except the basal ganglia (Sara 2009), whether the correlation between pupil dilation and IC/SCi/ACC is due to direct activation of these brain structures or due to a common input from LC to pupil and these brain structures remains unclear. Future work with reversible inactivation of the LC in behavior would be able to conclusively test this hypothesis.

Numerous works suggest that the pupil-linked arousal system contributes to the regulation of many cognitive factors in human behavior, including updating the internal model, learning, and serial choice bias (Eldar et al. 2013; Hong et al. 2014;

Nassar et al. 2012). We found that, when pupil size was large, the animals responded faster and became more liberal, indicated by more negative decision bias and therefore a higher tendency to respond. Consequently, a decoder constructed in this study had significantly greater than chance probability in predicting animals' behavior based on prestimulus pupil size. Moreover, pupil-linked arousal was likely reflective of the fluctuation of behavioral state. After a hit, pupil baseline size was typically higher, and animals were more likely to respond. On the contrary, after miss trials, the pupil baseline size was small, suggesting that the animal was in a low arousal state. Accordingly, the animal had low HR and FAR following miss trials.

Previous human studies provided mixed evidence regarding the relationship between baseline pupil size and reaction time in perceptual tasks (Gilzenrat et al. 2010; Hong et al. 2014; Murphy et al. 2011). We found a significant correlation between pupil baseline size and reaction time in our animals performing a tactile discrimination task. One possible explanation for this discrepancy is that task-related pupil dilation and reaction time may be mediated by distinct but interconnected neural circuitry (Urai et al. 2017). Reaction time is thought to be determined by evidence accumulation processes, which are at least partially mediated by prefrontal cortical areas (Brody et al. 2003; Gold and Shadlen 2007). Prefrontal cortex may also be involved in error detection (Yeung et al. 2004). In the above-mentioned studies, human subjects achieved near perfect performance on oddball tasks. On the contrary, our animals had ~30% FARs and 80% HRs. Therefore, neural circuitry monitoring errors, presumably in the prefrontal area, was likely to be activated during the task for our animals. Interestingly, the LC heavily projects to and receives projections from the prefrontal cortex (Berridge and Waterhouse 2003). Thus the interplay between the LC and prefrontal cortex is likely to mediate the correlation between reaction time and pupil baseline size that we observed in the present study. This would be an interesting topic of investigation for future work.

ACKNOWLEDGMENTS

The authors would like to thank Dr. Paul Sajda for constructive discussions and Edward Li for technical assistance in building the pupillometry system.

GRANTS

This work was supported by NIH R01MH112267.

DISCLOSURES

No conflicts of interest, financial or otherwise, are declared by the authors.

AUTHOR CONTRIBUTIONS

B.J.S., S.B., and Q.W. performed experiments; B.J.S. and Q.W. analyzed data; B.J.S. and Q.W. interpreted results of experiments; B.J.S. and Q.W. prepared figures; B.J.S. and Q.W. drafted manuscript; B.J.S. and Q.W. edited and revised manuscript; B.J.S., S.B., and Q.W. approved final version of manuscript; Q.W. conceived and designed research.

REFERENCES

Adbi M, Diamond ME, Arabzadeh E. Behavioral study of whisker-mediated vibration sensation in rats. *Proc Natl Acad Sci USA* 109: 971–976, 2012. doi:10.1073/pnas.1116726109.

- Andermann ML, Moore CI.** A somatotopic map of vibrissa motion direction within a barrel column. *Nat Neurosci* 9: 543–551, 2006. doi:10.1038/nrn1671.
- Aston-Jones G, Cohen JD.** An integrative theory of locus coeruleus-norepinephrine function: adaptive gain and optimal performance. *Annu Rev Neurosci* 28: 403–450, 2005. doi:10.1146/annurev.neuro.28.061604.135709.
- Bale MR, Petersen RS.** Transformation in the neural code for whisker deflection direction along the lemniscal pathway. *J Neurophysiol* 102: 2771–2780, 2009. doi:10.1152/jn.00636.2009.
- Berg RW, Kleinfeld D.** Rhythmic whisking by rat: retraction as well as protraction of the vibrissae is under active muscular control. *J Neurophysiol* 89: 104–117, 2003. doi:10.1152/jn.00600.2002.
- Berridge CW, Waterhouse BD.** The locus coeruleus-noradrenergic system: modulation of behavioral state and state-dependent cognitive processes. *Brain Res Brain Res Rev* 42: 33–84, 2003. doi:10.1016/S0165-0173(03)00143-7.
- Bishop CM.** *Pattern Recognition and Machine Learning (Information Science and Statistics)*. New York, NY: Springer-Verlag, 2006.
- Brecht M, Preilowski B, Merzenich MM.** Functional architecture of the mystacial vibrissae. *Behav Brain Res* 84: 81–97, 1997. doi:10.1016/S0166-4328(97)83328-1.
- Brody CD, Hernández A, Zainos A, Romo R.** Timing and neural encoding of somatosensory parametric working memory in macaque prefrontal cortex. *Cereb Cortex* 13: 1196–1207, 2003. doi:10.1093/cercor/bhg100.
- Bruno RM, Khatri V, Land PW, Simons DJ.** Thalamic cortical angular tuning domains within individual barrels of rat somatosensory cortex. *J Neurosci* 23: 9565–9574, 2003. doi:10.1523/JNEUROSCI.23-29-09565.2003.
- Brunton BW, Botvinick MM, Brody CD.** Rats and humans can optimally accumulate evidence for decision-making. *Science* 340: 95–98, 2013. doi:10.1126/science.1233912.
- Cano M, Bezdudnaya T, Swadlow HA, Alonso J-M.** Brain state and contrast sensitivity in the awake visual thalamus. *Nat Neurosci* 9: 1240–1242, 2006. doi:10.1038/nrn1760.
- Carter ME, Yizhar O, Chikahisa S, Nguyen H, Adamantidis A, Nishino S, Deisseroth K, de Lecea L.** Tuning arousal with optogenetic modulation of locus coeruleus neurons. *Nat Neurosci* 13: 1526–1533, 2010. doi:10.1038/nrn.2682.
- Carvell GE, Simons DJ.** Biometric analyses of vibrissal tactile discrimination in the rat. *J Neurosci* 10: 2638–2648, 1990. doi:10.1523/JNEUROSCI.10-08-02638.1990.
- Colizoli O, de Gee JW, Urai A, Donner TH.** Task-evoked pupil responses reflect internal belief states. *Cold Spring Harb. In press.* doi:10.1101/275776.
- de Gee JW, Knapen T, Donner TH.** Decision-related pupil dilation reflects upcoming choice and individual bias. *Proc Natl Acad Sci USA* 111: E618–E625, 2014. doi:10.1073/pnas.1317557111.
- de Gee JW, Colizoli O, Kloosterman NA, Knapen T, Nieuwenhuis S, Donner TH.** Dynamic modulation of decision biases by brainstem arousal systems. *eLife* 6: e23232, 2017. doi:10.7554/eLife.23232.
- Delis I, Dmochowski JP, Sajda P, Wang Q.** Correlation of neural activity with behavioral kinematics reveals distinct sensory encoding and evidence accumulation processes during active tactile sensing. *Neuroimage* 175: 12–21, 2018. doi:10.1016/j.neuroimage.2018.03.035.
- Diamond ME, von Heimendahl M, Knutsen PM, Kleinfeld D, Ahissar E.** ‘Where’ and ‘what’ in the whisker sensorimotor system. *Nat Rev Neurosci* 9: 601–612, 2008. doi:10.1038/nrn2411.
- Ebitz RB, Pearson JM, Platt ML.** Pupil size and social vigilance in Rhesus macaques. *Front Neurosci* 8: 100, 2014. doi:10.3389/fnins.2014.00100.
- Eldar E, Cohen JD, Niv Y.** The effects of neural gain on attention and learning. *Nat Neurosci* 16: 1146–1153, 2013. doi:10.1038/nrn.3428.
- Furuta T, Nakamura K, Deschenes M.** Angular tuning bias of vibrissa-responsive cells in the paralemniscal pathway. *J Neurosci* 26: 10548–10557, 2006. doi:10.1523/JNEUROSCI.1746-06.2006.
- Gerdjikov TV, Bergner CG, Stüttgen MC, Waiblinger C, Schwarz C.** Discrimination of vibrotactile stimuli in the rat whisker system: behavior and neurometrics. *Neuron* 65: 530–540, 2010. doi:10.1016/j.neuron.2010.02.007.
- Gilzenrat MS, Nieuwenhuis S, Jepma M, Cohen JD.** Pupil diameter tracks changes in control state predicted by the adaptive gain theory of locus coeruleus function. *Cogn Affect Behav Neurosci* 10: 252–269, 2010. doi:10.3758/CABN.10.2.252.
- Gold JJ, Shadlen MN.** The neural basis of decision making. *Annu Rev Neurosci* 30: 535–574, 2007. doi:10.1146/annurev.neuro.29.051605.113038.
- Gomez P, Ratcliff R, Perea M.** A model of the go/no-go task. *J Exp Psychol Gen* 136: 389–413, 2007. doi:10.1037/0096-3445.136.3.389.
- Harris KD, Thiele A.** Cortical state and attention. *Nat Rev Neurosci* 12: 509–523, 2011. doi:10.1038/nrn3084.
- Hartings JA, Temereanca S, Simons DJ.** High responsiveness and direction sensitivity of neurons in the rat thalamic reticular nucleus to vibrissa deflections. *J Neurophysiol* 83: 2791–2801, 2000. doi:10.1152/jn.2000.83.5.2791.
- Hartmann MJ, Johnson NJ, Towal RB, Assad C.** Mechanical characteristics of rat vibrissae: resonant frequencies and damping in isolated whiskers and in the awake behaving animal. *J Neurosci* 23: 6510–6519, 2003. doi:10.1523/JNEUROSCI.23-16-06510.2003.
- Hess EH, Polt JM.** Pupil size as related to interest value of visual stimuli. *Science* 132: 349–350, 1960. doi:10.1126/science.132.3423.349.
- Hess EH, Polt JM.** Pupil size in relation to mental activity during simple problem-solving. *Science* 143: 1190–1192, 1964. doi:10.1126/science.143.3611.1190.
- Hong L, Walz JM, Sajda P.** Your eyes give you away: prestimulus changes in pupil diameter correlate with poststimulus task-related EEG dynamics. *PLoS One* 9: e91321, 2014. doi:10.1371/journal.pone.0091321.
- Jadhav SP, Wolfe J, Feldman DE.** Sparse temporal coding of elementary tactile features during active whisker sensation. *Nat Neurosci* 12: 792–800, 2009. doi:10.1038/nrn.2328.
- Joshi S, Li Y, Kalwani RM, Gold JJ.** Relationships between pupil diameter and neuronal activity in the locus coeruleus, colliculi, and cingulate cortex. *Neuron* 89: 221–234, 2016. doi:10.1016/j.neuron.2015.11.028.
- Kaloti AS, Johnson EC, Bresee CS, Naufel SN, Perich MG, Jones DL, Hartmann MJ.** Representation of stimulus speed and direction in vibrissal-sensitive regions of the trigeminal nuclei: a comparison of single unit and population responses. *PLoS One* 11: e0158399, 2016. doi:10.1371/journal.pone.0158399.
- Krupa DJ, Wiest MC, Shuler MG, Laubach M, Nicolelis MAL.** Layer-specific somatosensory cortical activation during active tactile discrimination. *Science* 304: 1989–1992, 2004. doi:10.1126/science.1093318.
- Larsen RS, Waters J.** Neuromodulatory correlates of pupil dilation. *Front Neural Circuits* 12: 21, 2018. doi:10.3389/fncir.2018.00021.
- Lee CR, Margolis DJ.** Pupil dynamics reflect behavioral choice and learning in a Go/NoGo tactile decision-making task in mice. *Front Behav Neurosci* 10: 200, 2016. doi:10.3389/fnbeh.2016.00200.
- Lee SH, Simons DJ.** Angular tuning and velocity sensitivity in different neuron classes within layer 4 of rat barrel cortex. *J Neurophysiol* 91: 223–229, 2004. doi:10.1152/jn.00541.2003.
- Lee S-H, Dan Y.** Neuromodulation of brain states. *Neuron* 76: 209–222, 2012. doi:10.1016/j.neuron.2012.09.012.
- Lichtenstein SH, Carvell GE, Simons DJ.** Responses of rat trigeminal ganglion neurons to movements of vibrissae in different directions. *Somatosens Mot Res* 7: 47–65, 1990. doi:10.3109/08990229009144697.
- Liu Y, Rodenkirch C, Moskowitz N, Schriver B, Wang Q.** Dynamic lateralization of pupil dilation evoked by locus coeruleus activation results from sympathetic, not parasympathetic, contributions. *Cell Reports* 20: 3099–3112, 2017. doi:10.1016/j.celrep.2017.08.094.
- Mauri P, Miniussi C, Balconi M, Brignani D.** Bursts of transcranial electrical stimulation increase arousal in a continuous performance test. *Neuropsychologia* 74: 127–136, 2015. doi:10.1016/j.neuropsychologia.2015.03.006.
- McCormick DA, McGinley MJ, Salkoff DB.** Brain state dependent activity in the cortex and thalamus. *Curr Opin Neurobiol* 31: 133–140, 2015. doi:10.1016/j.conb.2014.10.003.
- McGinley MJ, David SV, McCormick DA.** Cortical membrane potential signature of optimal states for sensory signal detection. *Neuron* 87: 179–192, 2015a. doi:10.1016/j.neuron.2015.05.038.
- McGinley MJ, Vinck M, Reimer J, Batista-Brito R, Zaghera E, Cadwell CR, Tolia AS, Cardin JA, McCormick DA.** Waking state: rapid variations modulate neural and behavioral responses. *Neuron* 87: 1143–1161, 2015b. doi:10.1016/j.neuron.2015.09.012.
- Millard DC, Wang Q, Gollnick CA, Stanley GB.** System identification of the nonlinear dynamics in the thalamocortical circuit in response to patterned thalamic microstimulation in vivo. *J Neural Eng* 10: 066011, 2013. doi:10.1088/1741-2560/10/6/066011.

- Moradi F, Hipp C, Koch C.** Activity in the visual cortex is modulated by top-down attention locked to reaction time. *J Cogn Neurosci* 19: 331–340, 2007. doi:10.1162/jocn.2007.19.2.331.
- Murphy PR, Robertson IH, Balsters JH, O'Connell RG.** Pupillometry and P3 index the locus coeruleus-noradrenergic arousal function in humans. *Psychophysiology* 48: 1532–1543, 2011. doi:10.1111/j.1469-8986.2011.01226.x.
- Murphy PR, O'Connell RG, O'Sullivan M, Robertson IH, Balsters JH.** Pupil diameter covaries with BOLD activity in human locus coeruleus. *Hum Brain Mapp* 35: 4140–4154, 2014. doi:10.1002/hbm.22466.
- Murphy PR, Boonstra E, Nieuwenhuis S.** Global gain modulation generates time-dependent urgency during perceptual choice in humans. *Nat Commun* 7: 13526, 2016. doi:10.1038/ncomms13526.
- Musall S, Kaufman MT, Gluf S, Churchland A.** Movement-related activity dominates cortex during sensory-guided decision making. *Cold Spring Harb.* In press. doi:10.1101/308288
- Nassar MR, Rumsey KM, Wilson RC, Parikh K, Heasley B, Gold JL.** Rational regulation of learning dynamics by pupil-linked arousal systems. *Nat Neurosci* 15: 1040–1046, 2012. doi:10.1038/nn.3130.
- Niell CM, Stryker MP.** Modulation of visual responses by behavioral state in mouse visual cortex. *Neuron* 65: 472–479, 2010. doi:10.1016/j.neuron.2010.01.033.
- O'Connor DH, Clack NG, Huber D, Komiyama T, Myers EW, Svoboda K.** Vibrissa-based object localization in head-fixed mice. *J Neurosci* 30: 1947–1967, 2010a. doi:10.1523/JNEUROSCI.3762-09.2010.
- O'Connor DH, Peron SP, Huber D, Svoboda K.** Neural activity in barrel cortex underlying vibrissa-based object localization in mice. *Neuron* 67: 1048–1061, 2010b. doi:10.1016/j.neuron.2010.08.026.
- Ollerenshaw DR, Bari BA, Millard DC, Orr LE, Wang Q, Stanley GB.** Detection of tactile inputs in the rat vibrissa pathway. *J Neurophysiol* 108: 479–490, 2012. doi:10.1152/jn.00004.2012.
- Ollerenshaw DR, Zheng HJV, Millard DC, Wang Q, Stanley GB.** The adaptive trade-off between detection and discrimination in cortical representations and behavior. *Neuron* 81: 1152–1164, 2014. doi:10.1016/j.neuron.2014.01.025.
- Paxinos G, Watson C, Pennisi M, Topple A.** Bregma, lambda and the interaural midpoint in stereotaxic surgery with rats of different sex, strain and weight. *J Neurosci Methods* 13: 139–143, 1985. doi:10.1016/0165-0270(85)90026-3.
- Pinto DJ, Brumberg JC, Simons DJ.** Circuit dynamics and coding strategies in rodent somatosensory cortex. *J Neurophysiol* 83: 1158–1166, 2000. doi:10.1152/jn.2000.83.3.1158.
- Polack PO, Friedman J, Golshani P.** Cellular mechanisms of brain state-dependent gain modulation in visual cortex. *Nat Neurosci* 16: 1331–1339, 2013. doi:10.1038/nn.3464.
- Poulet JFA, Petersen CCH.** Internal brain state regulates membrane potential synchrony in barrel cortex of behaving mice. *Nature* 454: 881–885, 2008. doi:10.1038/nature07150.
- Rajkowski J, Majczynski H, Clayton E, Aston-Jones G.** Activation of monkey locus coeruleus neurons varies with difficulty and performance in a target detection task. *J Neurophysiol* 92: 361–371, 2004. doi:10.1152/jn.00673.2003.
- Reimer J, Froudarakis E, Cadwell CR, Yatsenko D, Denfield GH, Tolias AS.** Pupil fluctuations track fast switching of cortical states during quiet wakefulness. *Neuron* 84: 355–362, 2014. doi:10.1016/j.neuron.2014.09.033.
- Reimer J, McGinley MJ, Liu Y, Rodenkirch C, Wang Q, McCormick DA, Tolias AS.** Pupil fluctuations track rapid changes in adrenergic and cholinergic activity in cortex. *Nat Commun* 7: 13289, 2016. doi:10.1038/ncomms13289.
- Ritt JT, Andermann ML, Moore CI.** Embodied information processing: vibrissa mechanics and texture features shape micromotions in actively sensing rats. *Neuron* 57: 599–613, 2008. doi:10.1016/j.neuron.2007.12.024.
- Roedel A, Storch C, Holsboer F, Ohl F.** Effects of light or dark phase testing on behavioural and cognitive performance in DBA mice. *Lab Anim* 40: 371–381, 2006. doi:10.1258/002367706778476343.
- Sara SJ.** The locus coeruleus and noradrenergic modulation of cognition. *Nat Rev Neurosci* 10: 211–223, 2009. doi:10.1038/nrn2573.
- Schwarz C, Hentschke H, Butovas S, Haiss F, Stüttgen MC, Gerdjikov TV, Bergner CG, Waiblinger C.** The head-fixed behaving rat—procedures and pitfalls. *Somatosens Mot Res* 27: 131–148, 2010. doi:10.3109/08990220.2010.513111.
- Scott BB, Brody CD, Tank DW.** Cellular resolution functional imaging in behaving rats using voluntary head restraint. *Neuron* 80: 371–384, 2013. doi:10.1016/j.neuron.2013.08.002.
- Stanislaw H, Todorov N.** Calculation of signal detection theory measures. *Behav Res Methods Instrum Comput* 31: 137–149, 1999. doi:10.3758/BF03207704.
- Steriade M, McCormick DA, Sejnowski TJ.** Thalamocortical oscillations in the sleeping and aroused brain. *Science* 262: 679–685, 1993. doi:10.1126/science.8235588.
- Stringer C, Pachitariu M, Steinmetz N, Bai Reddy C, Carandini M, Harris KD.** Spontaneous behaviors drive multidimensional, brain-wide population activity. *Cold Spring Harb.* In press. doi:10.1101/306019.
- Stüttgen MC, Schwarz C.** Psychophysical and neurometric detection performance under stimulus uncertainty. *Nat Neurosci* 11: 1091–1099, 2008. doi:10.1038/nn.2162.
- Urai AE, Braun A, Donner TH.** Pupil-linked arousal is driven by decision uncertainty and alters serial choice bias. *Nat Commun* 8: 14637, 2017. doi:10.1038/ncomms14637.
- van den Brink RL, Murphy PR, Nieuwenhuis S.** Pupil diameter tracks lapses of attention. *PLoS One* 11: e0165274, 2016. doi:10.1371/journal.pone.0165274.
- Varazzani C, San-Galli A, Gilardeau S, Bouret S.** Noradrenaline and dopamine neurons in the reward/effort trade-off: a direct electrophysiological comparison in behaving monkeys. *J Neurosci* 35: 7866–7877, 2015. doi:10.1523/JNEUROSCI.0454-15.2015.
- Vilarchao ME, Estebanez L, Shulz DE, Férezou I.** Supra-barrel distribution of directional tuning for global motion in the mouse somatosensory cortex. *Cell Reports* 22: 3534–3547, 2018. doi:10.1016/j.celrep.2018.03.006.
- Vinck M, Batista-Brito R, Knoblich U, Cardin JA.** Arousal and locomotion make distinct contributions to cortical activity patterns and visual encoding. *Neuron* 86: 740–754, 2015. doi:10.1016/j.neuron.2015.03.028.
- von Heimendahl M, Itskov PM, Arabzadeh E, Diamond ME.** Neuronal activity in rat barrel cortex underlying texture discrimination. *PLoS Biol* 5: e305, 2007. doi:10.1371/journal.pbio.0050305.
- Wekselblatt JB, Niell CM.** Behavioral state—getting “in the zone”. *Neuron* 87: 7–9, 2015. doi:10.1016/j.neuron.2015.06.020.
- Wilent WB, Contreras D.** Dynamics of excitation and inhibition underlying stimulus selectivity in rat somatosensory cortex. *Nat Neurosci* 8: 1364–1370, 2005. doi:10.1038/nn1545.
- Wolfe J, Hill DN, Pahlavan S, Drew PJ, Kleinfeld D, Feldman DE.** Texture coding in the rat whisker system: slip-stick versus differential resonance. *PLoS Biol* 6: e215, 2008. doi:10.1371/journal.pbio.0060215.
- Yang M, Weber MD, Crawley JN.** Light phase testing of social behaviors: not a problem. *Front Neurosci* 2: 186–191, 2008. doi:10.3389/neuro.01.029.2008.
- Yerkes RM, Dodson JD.** The relation of strength of stimulus to rapidity of habit-formation. *J Comp Neurol Psychol* 18: 459–482, 1908. doi:10.1002/cne.920180503.
- Yeung N, Botvinick MM, Cohen JD.** The neural basis of error detection: conflict monitoring and the error-related negativity. *Psychol Rev* 111: 931–959, 2004. doi:10.1037/0033-295X.111.4.931.
- Yu AJ, Dayan P.** Uncertainty, neuromodulation, and attention. *Neuron* 46: 681–692, 2005. doi:10.1016/j.neuron.2005.04.026.
- Zhang Q, Kong L, Jiang Y.** The interaction of arousal and valence in affective priming: behavioral and electrophysiological evidence. *Brain Res* 1474: 60–72, 2012. doi:10.1016/j.brainres.2012.07.023.
- Zheng HJV, Wang Q, Stanley GB.** Adaptive shaping of cortical response selectivity in the vibrissa pathway. *J Neurophysiol* 113: 3850–3865, 2015. doi:10.1152/jn.00978.2014.